Decode-and-Forward Relaying for Cooperative NOMA Systems With Direct Links

Hongwu Liu, *Member, IEEE*, Zhiguo Ding, *Senior Member, IEEE*, Kyeong Jin Kim, *Senior Member, IEEE*, Kyung Sup Kwak, *Member, IEEE*, and H. Vincent Poor, *Fellow, IEEE*

***Abstract*— This paper investigates a cooperative non-orthogonal multiple access system, in which a base station communicates with two far users with the aid of a decode-and-forward (DF) relay. Three cooperative relaying schemes, namely, the fixed relaying (FR), the selective DF with coordinated direct and relay transmission (SDF-CDRT), and the incremental-selective DF (ISDF) relaying are proposed to enhance the outage performance for the two far users by utilizing both the direct and relay links. Taking into account the received signal-to-noise ratio (SNR) events at the relay, the SDF-CDRT scheme adaptively forms an orthogonal transmission branch with respect to the direct link or keeps silent to reduce error propagation. Besides considering the relay detection results, the ISDF scheme further exploits the limited feedback of the received SNR events from two users, so that error propagation can be avoided and unnecessary relaying can be reduced. Analytical expressions for the outage probabilities and average throughputs of the paired users are derived in closed-form for the three cooperative relaying schemes. Asymptotic expressions for the outage probabilities are derived in the high SNR region. It is shown that the FR and SDF-CDRT schemes achieve a diversity order of one for both users, while the ISDF scheme achieves a diversity order of two for both users. The superior system performance achieved by the proposed schemes over those of the existing methods is verified by Monte Carlo simulations.**

***Index Terms*— Non-orthogonal multiple access, decode-and-forward, selective relaying, outage probability.**

Manuscript received December 21, 2017; revised September 23, 2018; accepted September 25, 2018. Date of publication October 11, 2018; date of current version December 10, 2018. This work was supported in part by the National Research Foundation of Korea through the Korean Government (Ministry of Science, ICT, and Future Planning) under Grant NRF-2017R1A2B2012337 and in part by the U.S. National Science Foundation under Grant CNS-1702808. The work of Z. Ding was supported in part by U.K. EPSRC under Grant EP/P009719/2 and in part by H2020-MSCA-RISE-2015 Project under Grant 690750. The associate editor coordinating the review of this paper and approving it for publication was A. Zaidi. *(Corresponding authors: Hongwu Liu; Kyung Sup Kwak.)*

H. Liu is with the School of Information Science and Electrical Engineering, Shandong Jiaotong University, Jinan 250357, China (e-mail: hong.w.liu@hotmail.com).

Z. Ding is with the School of Electrical and Electronic Engineering, The University of Manchester, Manchester M13 9PL, U.K. (e-mail: zhiguo.ding@manchester.ac.uk).

K. J. Kim is with Mitsubishi Electric Research Laboratories, Cambridge, MA 02139 USA (e-mail: keyong.j.kim@hotmail.com).

K. S. Kwak is with the Department of Information and Communication Engineering, Inha University, Incheon 22212, South Korea (e-mail: kskwak@inha.ac.kr).

H. V. Poor is with the Department of Electrical Engineering, Princeton University, Princeton, NJ 08544 USA (e-mail: poor@princeton.edu).

Color versions of one or more of the figures in this paper are available online at http://ieeexplore.ieee.org.

Digital Object Identifier 10.1109/TWC.2018.2873999

I. Introduction

DUE to its superior spectral efficiency and its capability to support massive connectivity, non-orthogonal multiple access (NOMA) has been envisioned as a promising multiple access candidate for fifth generation (5G) networks [1]–[3]. In particular, power-domain NOMA can serve multiple users for demanding large-scale heterogeneous traffic by using the same time/frequency/code resource but with different power levels [3], [4]. As a special case of NOMA, multiple user superposition transmission (MUST) has been proposed for 3GPP long term evolution (LTE) [5], [6]. To exploit channel conditions of different users opportunistically, users with poorer channel qualities are allocated more transmit power in NOMA systems, while users with better channel qualities are less allocated. In this way, both poorer-channel and better-channel users can decode their messages successfully at the cost of applying successive interference cancellation (SIC) at better-channel users. It has shown that NOMA is more power efficient than conventional orthogonal multiple access (OMA) when users are properly grouped according to their channel qualities or quality of service (QoS) requirements [7]–[10].

Recently, cooperative NOMA schemes incorporating relaying have been proposed in the literature to strengthen system performances. The first cooperative NOMA scheme was proposed in [2], where a user with strong channel conditions was used as a relay beside decoding its own message via SIC. In [11], a dedicated multi-antenna amplify-and-forward (AF) relay was introduced to aid transmissions from a base station (BS) to NOMA users. Considering perfect and imperfect knowledge of channel state information (CSI), the performances of cooperative NOMA systems with an AF relay under Nakagami-m fading were studied in [12] and [13], respectively. A partial relay selection (RS) was proposed in [14], where several AF relay criteria were proposed to assist the BS-to-users transmissions. Furthermore, the authors in [15] proposed a two-stage AF RS scheme, which achieves a diversity order the same as the number of the relay nodes. The two-stage RS schemes have also been investigated for NOMA decode-and-forward (DF) systems to decrease outage probability and obtain spatial diversity in [15] and [16]. To enhance cell edge coverage, multiple antennas have been employed at the DF relay and users for cooperative NOMA systems [17]. Based on the user-aided relay and dedicated relay, several full-duplex relaying schemes have been proposed for cooperative NOMA DF systems in [18]–[21].

In [22] and [23], cooperative NOMA transmissions have been combined with simultaneous wireless information and power transfer.

When direct links between the BS and users are non-negligible, coordinated transmissions incorporating direct links can significantly enhance the performance of cooperative NOMA systems [14], [18], [19], [24], [25]. Direct links exist widely in not only the overlapping of macro and micro cells [14], [24], but also device-to-device (D2D) communications [19], [25]. Compared to the conventional NOMA-DF scheme adopted in [15]–[17], the coordinated direct and relay transmission (CDRT) scheme achieves the improved outage performance and increased ergodic sum rate [24]. However, in coordinated transmissions, a main challenge is to acquire side information for interference cancellation, which may result in huge overhead due to massive connectivity in cooperative NOMA systems. Another issue in the current CDRT schemes is that the users are paired based on channel quality, so that the far user always achieves a low-rate transmission. Currently, the CDRT schemes designed for aiding two far users can be recognized as the novel contribution. It is also worthwhile to point out that the existences of direct links are commonly assumed in multiple access relay channels (MARCs) for downlink and uplink transmissions [26]–[31]. In [26], the authors proposed a reverse compute-and-forward (CF) relaying scheme for the dowlink MARCs under an error-free and capacity-limited souce-to-relay channel. For the uplink MARCs with solid relay-to-destination links, the CF relaying scheme for two user access was investigated in [27] and lately extended to the scenario with multiuser and multiple relays in [28].

On the other hand, when direct links are available in cooperative systems, adaptive relaying schemes such as the selective relaying and incremental relaying can be applied to reduce error propagation resulted from the detection failure at the relay [32]–[36]. As a simple way to reduce error propagation for cooperative systems, the selective DF (SDF) relaying makes a decision whether it operates in the DF mode or keeps silent based on a received signal-to-noise ratio (SNR) threshold at the relay, so that the end-to-end performance can be improved [32], [33]. By exploiting the limited SNR feedback from the destination, the authors in [34] proposed the incremental relaying with a significant improvement of spectrum efficiency over the conventional fixed relaying (FR) and SDF relaying schemes. The outage probability and end-to-end performance of the incremental relaying have been investigated in [35] and [36], respectively. In [37], the authors proposed the incremental-selective DF (ISDF) relaying by combining incremental relaying and SDF relaying, which achieved an improved system performance over that of the simple incremental DF relaying. Several hybrid relaying schemes that combine SDF, AF, and incremental relaying have been investigated in [38]–[40]. However, to the best knowledge of the authors, selective relaying and incremental relaying have not been applied for cooperative NOMA systems taking into account the superposition in the power domain for multiple access.

In this paper, we consider a cooperative NOMA system with one BS communicating with two far receivers with the aid of an intermediate relay. Different from existing works on MARCs where the CF relaying is applied, we assume that the relay operates in the DF mode and investigate cooperative relaying taking into account both the direct and relay links. The main contributions of this paper are summarized as follows.

- In the presence of direct links, three cooperative relaying schemes, i.e., the FR, SDF with CDRT (SDF-CDRT), and ISDF schemes, are individually investigated for the cooperative NOMA system. Compared to most existing cooperative NOMA schemes incorporating a single direct link to the near user [18], [19], [24], [25], our work considers the direct links from the BS to two far users, so that two far users with different QoS requirements can be paired with each other and get benefit from cooperative relaying. In contrast to cooperative NOMA systems where the direct links from the BS to the far users are unavailable, the proposed cooperative relaying schemes significantly improve the outage performance by taking advantages of both the direct and relay links.
- To reduce error propagation resulted from the detection failures at the relay, the SDF-CDRT scheme is designed to switch the relaying on or off depending on the received SNRs at the relay. When the received SNRs at the relay are high enough to ensure the correct detection, the SDF-CDRT scheme forms an orthogonal branch with respect to the direct link transmissions, so that only linear combination is applied at each receiver and the decoding complexity can be reduced in such a case. When the received SNRs cannot ensure the correct detection for the superposition, the relay keeps silent and the BS starts a new transmission block, which takes the advantages provided by the SDF relaying scheme [32], [33]. Based on limited information feedback of the received SNR events from two users, the ISDF scheme switches the relaying on or off depending on the combinations of the received SNR events at the relay and two users. Accordingly, the unnecessary relaying can be reduced by the ISDF scheme over the SDF scheme.
- For the FR, SDF-CDRT, and ISDF schemes, the closed-form expressions for the outage probabilities are derived for both two users. To highlight the impact of the system parameters on the outage performance, asymptotic outage probabilities achieved at both two users are derived for the three proposed cooperative relaying schemes, respectively. It is shown that the FR and SDF-CDRT schemes achieve a diversity order of one for both two users, whereas the ISDF scheme provides a diversity gain order of two for the two users' case. Taking into account the additional time slots consumed for relaying, the analytical results for the average throughputs are derived for the FR, SDF-CDRT, and ISDF schemes, respectively.

The rest of this paper is organized as follows: Section II presents the system model, the FR scheme, and the SDF-CDRT scheme; Section III presents the ISDF scheme.

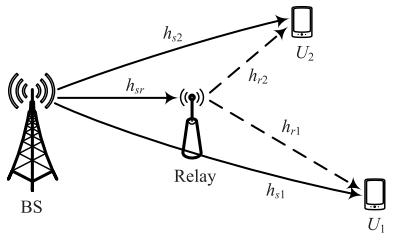

Fig. 1. System model of the cooperative NOMA system with a DF relay.

Section IV derives the outage probabilities for the three proposed cooperative relaying schemes and conducts asymptotic outage performance analyses; Section V gives simulation results to verify the superior performance achieved by the proposed cooperative relaying schemes and Section VI summarizes the paper.

II. System Model and Simple Relaying Schemes

We consider a downlink cooperative NOMA system consisting of a BS, a DF relay, and two far users. The system model is depicted in Fig. 1, in which the two far users are denoted by U_1 and U_2, respectively. We assume that all the nodes are equipped with a single antenna and work in the half-duplex mode. In the considered system, the BS and relay can be the transmitters of a macro cell and a micro cell, respectively, and we assume that the direct links from the BS to two users are non-negligible. The considered system model can also be applied for D2D communications [25], in which the relay can be a device in the proximity of the two users and we also assume that the direct links from the BS to the two users exist. The channels from the BS to the relay, from the BS to U_i, and from the relay to U_i are denoted by h_{sr}, h_{si}, and h_{ri}, respectively, with $i = 1$ and 2. All the channels are modeled as independent but non-identically distributed (i.n.i.d.) complex Gaussian random variables (RVs) with zero means and variances β_{sr}, β_{si}, and β_{ri} for h_{sr}, h_{si}, and h_{ri}, respectively. Moreover, all the channels are assumed to be block fading, i.e., a channel keeps constant during one transmission block and can vary from one transmission block to another. The additive white Gaussian noises (AWGNs) at all the receivers are assumed to have zero mean and variance σ^2, while the information signal for U_i is denoted by x_i satisfying $\mathbb{E}\{x_i\} = 0$ and $\mathbb{E}\{|x_i|^2\} = 1$.

In cooperative NOMA systems, users can be ordered by their channel qualities, which in turn determines the decoding order at the receiver side and results in a huge overhead for the case with a large number of users. Another user pairing criterion is to order users according to their QoS requirements [15], [16], which enables grouping users even if they have statistically the same channel qualities. Moreover, the CSI acquirements at the transmitters can be significantly reduced if QoS-based user pairing is applied [15]. In this paper, we also apply QoS-based user pairing and assume that user U_1 is a low target rate device but requiring a timely service, while user U_2 is more delay-tolerated than user U_1 but needs a higher throughput.

TABLE I
Received SNR Events and Detection Results at the Relay

Received SNR event	Detection result
$\varepsilon_1 := (\gamma_r^{x_1} \geq \gamma_{\mathrm{th},1}) \cap (\gamma_r^{x_2} \geq \gamma_{\mathrm{th},2})$	Correct x_1 and x_2
$\varepsilon_2 := (\gamma_r^{x_1} \geq \gamma_{\mathrm{th},1}) \cap (\gamma_r^{x_2} < \gamma_{\mathrm{th},2})$	Correct x_1 and incorrect x_2
$\varepsilon_3 := \gamma_r^{x_1} < \gamma_{\mathrm{th},1}$	Incorrect x_1 and x_2

In the considered system, each downlink transmission block can be accomplished within two time slots. In the first time slot, the BS broadcasts the superposed signal $x_b \triangleq \sqrt{\alpha_1}x_1 + \sqrt{\alpha_2}x_2$ to all the other nodes, where α_i is the power allocation coefficient, which satisfies $\sum_{i=1}^{2}\alpha_i = 1$ and $\alpha_i > 0$. The received signals at the relay and U_i are respectively given by

$$y_r = h_{sr}\big(\sqrt{\alpha_1 P_s}x_1 + \sqrt{\alpha_2 P_s}x_2\big) + n_r \tag{1}$$

and

$$y_i^{(1)} = h_{si}\big(\sqrt{\alpha_1 P_s}x_1 + \sqrt{\alpha_2 P_s}x_2\big) + n_i^{(1)}, \tag{2}$$

where P_s is the transmit power, n_r and $n_i^{(1)}$ are the AWGNs at the relay and U_i, respectively. Since we assume that the QoS requirements of U_1 are much less demanding than those of U_2, the decoding order at the relay is always from U_1 to U_2 [15]. Therefore, the received SNRs at the relay for decoding x_1 and x_2 can be respectively expressed as

$$\gamma_r^{x_1} = \frac{\alpha_1\rho|h_{sr}|^2}{\alpha_2\rho|h_{sr}|^2 + 1} \quad \text{and } \gamma_r^{x_2} = \alpha_2\rho|h_{sr}|^2, \tag{3}$$

where $\rho \triangleq P_s/\sigma^2$ is the transmit SNR.

A. FR Scheme

In this subsection, we investigate the conventional FR scheme which utilizes both the direct and relay link transmissions to enhance the detection performance at the receiver side. After correct detecting x_1 and x_2, the relay regenerates and forwards the superposition x_b, so that the received signal at U_i in the second time slot can be expressed as

$$y_i^{(2)} = h_{ri}\big(\sqrt{\alpha_1 P_r}x_1 + \sqrt{\alpha_2 P_r}x_2\big) + n_i^{(2)}, \tag{4}$$

where P_r is the relaying transmit power and $n_i^{(2)}$ is the AWGN at U_i in the second time slot. It is worthwhile to point out that the above signal model strictly relies on the correct detection at the relay. When the source-to-relay link suffers deep fading, the relay may not always detect x_1 and x_2 correctly. In Table I, three detection results and corresponding received SNR events at the relay are presented, where $\gamma_{\mathrm{th},i} \triangleq 2^{R_i} - 1$ is the required SNR threshold for correct detecting x_i with R_i denoting the target transmission rate of U_i. In the FR scheme, each user applies maximum ratio combining (MRC) to recover its desired signal. The MRC processing and the end-to-end received SNRs at U_1 and U_2 are discussed as follows.

1) Event ε_1: For each user, MRC is applied to (2) and (4) at the receiver side to recover its desired signal. When the event ε_1 occurs, the relay can correctly forward x_b, so that the end-to-end received SNR at U_1 for detecting x_1 is given by

$$\gamma_{1,\,\mathrm{fr}}^{x_1}(\varepsilon_1) = \frac{\alpha_1\rho(|h_{s1}|^2 + |\tilde{h}_{r1}|^2)}{\alpha_2\rho(|h_{s1}|^2 + |\tilde{h}_{r1}|^2) + 1}, \tag{5}$$

where $\tilde{h}_{r1} \triangleq \sqrt{\chi}h_{r1}$ with $\chi \triangleq P_r/P_s$. At U_2, MRC is also applied to (2) and (4) for detecting x_1. Then, SIC is performed for detecting x_2. The end-to-end received SNRs at U_2 for detecting x_1 and x_2 can be respectively expressed as

$$\gamma_{2,\,\mathrm{fr}}^{x_1}(\varepsilon_1) = \frac{\alpha_1\rho(|h_{s2}|^2 + |\tilde{h}_{r2}|^2)}{\alpha_2\rho(|h_{s2}|^2 + |\tilde{h}_{r2}|^2) + 1} \tag{6}$$

and

$$\gamma_{2,\,\mathrm{fr}}^{x_2}(\varepsilon_1) = \alpha_2\rho(|h_{s2}|^2 + |\tilde{h}_{r2}|^2). \tag{7}$$

2) Event ε_2: When the event ε_2 occurs, we have $\gamma_{1,\mathrm{fr}}^{x_1}(\varepsilon_2) = \gamma_{1,\mathrm{fr}}^{x_1}(\varepsilon_1)$ and $\gamma_{2,\,\mathrm{fr}}^{x_1}(\varepsilon_2) = \gamma_{2,\mathrm{fr}}^{x_1}(\varepsilon_1)$ due to the correct forwarding of $\sqrt{\alpha_1}x_1$ by the relay. However, the relay forwards the incorrect $\sqrt{\alpha_2}x_2$ in this case, so that the end-to-end received SNR for U_2 to detect x_2 becomes

$$\gamma_{2,\,\mathrm{fr}}^{x_2}(\varepsilon_2) = \frac{\alpha_2\rho|h_{s2}|^2}{\alpha_2\rho|\tilde{h}_{r2}|^2 + 1}. \tag{8}$$

Compared to (7), we can see that the end-to-end received SNR in (8) becomes smaller.

3) Event ε_3: When the event ε_3 occurs, neither x_1 nor x_2 is correctly forwarded by the relay, so that the end-to-end received SNRs at U_1 and U_2 degrade to

$$\gamma_{1,\,\mathrm{fr}}^{x_1}(\varepsilon_3) = \frac{\alpha_1\rho|h_{s1}|^2}{\alpha_2\rho|h_{s1}|^2 + \rho|\tilde{h}_{r1}|^2 + 1}, \tag{9}$$

$$\gamma_{2,\,\mathrm{fr}}^{x_1}(\varepsilon_3) = \frac{\alpha_1\rho|h_{s2}|^2}{\alpha_2\rho|h_{s2}|^2 + \rho|\tilde{h}_{r2}|^2 + 1}, \tag{10}$$

and

$$\gamma_{2,\,\mathrm{fr}}^{x_2}(\varepsilon_3) = \frac{\alpha_2\rho|h_{s2}|^2}{\rho|\tilde{h}_{r2}|^2 + 1}. \tag{11}$$

The expressions in (5)-(11) show that the end-to-end received SNRs are heavily affected by the detection results at the relay. When the events ε_2 and ε_3 occur, error propagation is unavoidable, which decreases the end-to-end received SNRs at U_1 and U_2. In order to reduce error propagation when the events ε_2 and ε_3 occur and to avoid SIC when ε_1 occurs, we propose the SDF-CDRT scheme in the next subsection.

B. SDF-CDRT Scheme

Based on a certain received SNR threshold at the relay, the SDF relaying is a simple way to reduce error propagation for cooperative relaying systems [33]. In this section, we propose an SDF-CDRT scheme for the considered cooperative NOMA systems. In the SDF-CDRT scheme, when the event ε_1 occurs, the relay generates a new superposition such that an orthogonal structure is formed with respect to the direct and relay transmissions. Consequently, linear combining is applied at each receiver to recover the desired signal and SIC can be avoided in such a case. Moreover, when ε_2 or ε_3 occurs, the relay keeps silent, so that error propagation resulted from the failure detection at the relay can be avoided and spectral efficiency can be improved by a new block transmission via the BS [33].

In the SDF-CDRT scheme, the BS broadcasts x_b to the relay and two users in the first time slot. The operation procedure of the SDF-CDRT scheme in the second time slot and the end-to-end received SNRs at U_1 and U_2 are described as follows.

1) Event ε_1: When the event ε_1 occurs, the relay generates a new superposition

$$x_r = \sqrt{\alpha_2}x_1 - \sqrt{\alpha_1}x_2 \tag{12}$$

for its transmission in the second time slot. Then, the received signal at U_i in the second time slot is given by

$$y_i^{(2)} = h_{ri}\big(\sqrt{\alpha_2 P_r}x_1 - \sqrt{\alpha_1 P_r}x_2\big) + n_i^{(2)}. \tag{13}$$

For each user, the received signals from both the first and second time slots can be rewritten in a matrix form as

$$\begin{bmatrix} \dfrac{y_i^{(1)}}{h_{si}\sqrt{P_s}} \\ \dfrac{y_i^{(2)}}{h_{ri}\sqrt{P_r}} \end{bmatrix} = \underbrace{\begin{bmatrix} \sqrt{\alpha_1} & \sqrt{\alpha_2} \\ \sqrt{\alpha_2} & -\sqrt{\alpha_1} \end{bmatrix}}_{\mathcal{H}} \begin{bmatrix} x_1 \\ x_2 \end{bmatrix} + \begin{bmatrix} \dfrac{n_i^{(1)}}{h_{si}\sqrt{P_s}} \\ \dfrac{n_i^{(2)}}{h_{ri}\sqrt{P_r}} \end{bmatrix}, \tag{14}$$

where $\mathcal{H}$ is the equivalent power allocation matrix. Different from the 2×2 orthogonal design for space-time block coding (STBC) [41], where $\mathcal{H}$ contains the complex space-time channel coefficients weighted by ± 1, the proposed power allocation matrix is a 2×2 real matrix, which avoids the conjugate of the signal in the power-domain. In general, $\mathcal{H}$ can be in any form of the 2×2 rotation or reflection, i.e.,

$$\mathcal{H} = \begin{bmatrix} \cos\theta & -\sin\theta \\ \sin\theta & \cos\theta \end{bmatrix} \text{ or } \mathcal{H} = \begin{bmatrix} \cos\theta & \sin\theta \\ \sin\theta & -\cos\theta \end{bmatrix}, \tag{15}$$

where $\theta \in (0, \pi/2)$. Thus, the power allocation can be interpreted as a rotation or reflection of $[x_1, x_2]^T$. It can be shown that $\mathcal{H}$ is an orthogonal matrix with a unit norm for each of its row, so that it not only satisfies the power constraint $\alpha_1^2 + \alpha_2^2 = 1$, but also provides the orthogonality for the proposed SDF-CDRT scheme. Without loss of generality, we adopt the reflection form (14) in the sequential. To recover the desired singal, each user applies linear combining to its received signals from both the first and second time slots. Specifically, U_1 and U_2 apply the linear combinations as

$$\begin{aligned} \breve{x}_1 &= y_1^{(1)}\sqrt{\alpha_1}\tilde{h}_{r1} + y_1^{(2)}\sqrt{\alpha_2}h_{s1} \\ &= h_{s1}\tilde{h}_{r1}\sqrt{P}x_1 + \sqrt{\alpha_1}\tilde{h}_{r1}n_1^{(1)} + \sqrt{\alpha_2}h_{s1}n_1^{(2)} \end{aligned} \tag{16}$$

and

$$\begin{aligned} \breve{x}_2 &= y_2^{(1)}\sqrt{\alpha_2}\tilde{h}_{r2} - y_2^{(2)}\sqrt{\alpha_1}h_{s2} \\ &= h_{s2}\tilde{h}_{r2}\sqrt{P}x_2 + \sqrt{\alpha_2}\tilde{h}_{r2}n_2^{(1)} - \sqrt{\alpha_1}h_{s2}n_2^{(2)} \end{aligned} \tag{17}$$

for detecting x_1 and x_2, respectively. Based on (16) and (17), the end-to-end received SNRs at U_1 and U_2 for detecting x_1 and x_2 can be respectively expressed as

$$\gamma_{1,\mathrm{sdf-cdrt}}^{x_1}(\varepsilon_1) = \frac{\rho|h_{s1}|^2|\tilde{h}_{r1}|^2}{\alpha_1|\tilde{h}_{r1}|^2 + \alpha_2|h_{s1}|^2} \tag{18}$$

and

$$\gamma_{2,\mathrm{sdf-cdrt}}^{x_2}(\varepsilon_1) = \frac{\rho|h_{s2}|^2|\tilde{h}_{r2}|^2}{\alpha_1|h_{s2}|^2 + \alpha_2|\tilde{h}_{r2}|^2}. \tag{19}$$

2) Event ε_2 or ε_3: When the event ε_2 or ε_3 occurs, the relay cannot correctly regenerate x_r. In such a case, the relay keeps silent and the BS needs to start a new superposition transmission [33]. At each receiver, the detection is based on the received signal in the first time slot. Thus, when ε_i $(i = 2, 3)$ occurs, the end-to-end received SNRs at U_1 and U_2 are respectively given by

$$\gamma_{1,\mathrm{sdf-cdrt}}^{x_1}(\varepsilon_i) = \frac{\alpha_1\rho|h_{s1}|^2}{\alpha_2\rho|h_{s1}|^2 + 1}, \tag{20}$$

$$\gamma_{2,\mathrm{sdf-cdrt}}^{x_1}(\varepsilon_i) = \frac{\alpha_1\rho|h_{s2}|^2}{\alpha_2\rho|h_{s2}|^2 + 1}, \tag{21}$$

and

$$\gamma_{2,\mathrm{sdf-cdrt}}^{x_2}(\varepsilon_i) = \frac{\alpha_1\rho|h_{s1}|^2}{\alpha_2\rho|h_{s1}|^2 + 1}. \tag{22}$$

Compared to the conventional FR scheme, the SDF-CDRT scheme forms an orthogonal transmission branch with respect to the direct link when ε_1 occurs. When either ε_2 or ε_3 occurs, the SDF-CDRT scheme stops relaying, so that error propagation can be avoided. However, when ε_1 occurs, the SDF-CDRT scheme always operates in the DF mode no matter what the direct links' qualities are, which results in unnecessary relaying if U_i can recover its desired signal via the direct link transmission. Motivated by this, we propose the ISDF relaying scheme in the next section.

III. ISDF Relaying

By exploiting the limited SNR feedback from the receiver to the BS and relay, the incremental relaying can significantly improve reception reliability over the fixed and selective relaying schemes for point-to-point communication systems [34]–[36]. However, due to the superposition in the power-domain for multiple access, the feedback of the received SNRs in the considered system is much more complicated than that of a point-to-point communication system. In the case that two users are grouped for multiple access, there are six combinations of the received SNR events with respect to the detection results at U_1 and U_2 in delay-limited transmissions based on the proposed ISDF relaying scheme.

In the ISDF scheme, the BS broadcasts a superposition x_b in the first time slot. Then, the received SNR events at U_1 and U_2 are fed back to the relay, based on which the relay makes a preliminary decision on whether it forwards a signal/superposition or not. If the preliminary decision is to forward, the relay further checks whether its received SNRs are high enough to correctly regenerate the required signal. Only when the required signal/superposition can be regenerated correctly, the relay forwards the signal/superposition; otherwise, the relay keeps silent and the BS starts a new transmission [34]–[36].

The preliminary decision rule at the relay is presented in Table II, which is designed to forward a signal to either U_1, U_2, or both if it is necessary. In Table II, the received SNR events at U_1 and U_2 are defined as

TABLE II
PRELIMINARY DECISION RULE FOR THE ISDF RELAYING

Decision (U_1 \ U_2)	$\tilde{\varepsilon}_1$	$\tilde{\varepsilon}_2$	$\tilde{\varepsilon}_3$
$\hat{\varepsilon}_1$	Silent	x_2	x_b
$\hat{\varepsilon}_2$	x_1	x_b	x_b

$$\begin{aligned}
&\hat{\varepsilon}_1 := \gamma_1^{x_1} \geq \gamma_{\mathrm{th},1},\\
&\hat{\varepsilon}_2 := \gamma_1^{x_1} < \gamma_{\mathrm{th},1},\\
&\tilde{\varepsilon}_1 := (\gamma_2^{x_1} \geq \gamma_{\mathrm{th},1}) \cap (\gamma_2^{x_2} \geq \gamma_{\mathrm{th},2}),\\
&\tilde{\varepsilon}_2 := (\gamma_2^{x_1} \geq \gamma_{\mathrm{th},1}) \cap (\gamma_2^{x_2} < \gamma_{\mathrm{th},2}), \quad \text{and}\\
&\tilde{\varepsilon}_3 := \gamma_2^{x_1} < \gamma_{\mathrm{th},1},
\end{aligned} \tag{23}$$

where $\gamma_1^{x_1}$ is the received SNR at U_1 in the first time slot for detecting x_1, which is given by

$$\gamma_1^{x_1} = \frac{\alpha_1\rho|h_{s1}|^2}{\alpha_2\rho|h_{s1}|^2 + 1}. \tag{24}$$

Moreover, $\gamma_2^{x_1}$ and $\gamma_2^{x_2}$ are the received SNRs at U_2 in the first time slot for detecting x_1 and x_2, respectively, which are respectively given by

$$\gamma_2^{x_1} = \frac{\alpha_1\rho|h_{s2}|^2}{\alpha_2\rho|h_{s2}|^2 + 1} \tag{25}$$

and

$$\gamma_2^{x_2} = \alpha_2\rho|h_{s2}|^2. \tag{26}$$

After a preliminary decision is made, the relay further evaluates its received SNRs and makes a formal decision on whether it operates in the DF relaying mode or keeps silent according to the formal decision rule provided in Table III. Note that Table III is extended from Table II by taking into account the received SNR events at the relay. For example, when the events $\{\hat{\varepsilon}_2, \tilde{\varepsilon}_2\}$ occur, the preliminary rule is to make the relay forward x_b according to Table II. In such a case, the relay further checks which one of $\{\varepsilon_1, \varepsilon_2, \varepsilon_3\}$ occurs to make the formal decision. If ε_1 occurs, the relay can forward x_b. However, if ε_2 occurs, the relay can only forward x_1 due to its failure detection of x_2. As such, when ε_3 occurs, the relay keeps silent even if the events $\{\hat{\varepsilon}_2, \tilde{\varepsilon}_2\}$ occur. At the receiver side, we assume that each user can acquire the indication knowledge of the forwarded signal, i.e., which signal of $\{x_1, x_2, x_b\}$ is forwarded, so that MRC can be performed adaptively at each receiver. The end-to-end received SNRs achieved by the ISDF scheme are discussed as follows.

A. Events $\{\varepsilon_1, \hat{\varepsilon}_1, \tilde{\varepsilon}_2\}$

According to Table III, when $\{\varepsilon_1, \hat{\varepsilon}_1, \tilde{\varepsilon}_2\}$ occurs, the relay only forwards x_2 with its full transmit power to help U_2. For U_1, its end-to-end received SNR is determined by its

TABLE III
FORMAL DECISION RULE AT THE RELAY

Decision / Feedback / Relay's SNR	$\{\hat{\varepsilon}_1, \tilde{\varepsilon}_1\}$	$\{\hat{\varepsilon}_1, \tilde{\varepsilon}_2\}$	$\{\hat{\varepsilon}_1, \tilde{\varepsilon}_3\}$	$\{\hat{\varepsilon}_2, \tilde{\varepsilon}_1\}$	$\{\hat{\varepsilon}_2, \tilde{\varepsilon}_2\}$	$\{\hat{\varepsilon}_2, \tilde{\varepsilon}_3\}$
ε_1	Silent	x_2	x_b	x_1	x_b	x_b
ε_2	Silent	Silent	x_1	x_1	x_1	x_1
ε_3	Silent	Silent	Silent	Silent	Silent	Silent

TABLE IV
FEEDBACK AND SIGNALING REQUIRED BY THE RELAYING SCHEMES

Relaying scheme	Received SNR event feedback	Signaling for detecting
FR	Null	One bit for indicating either the BS or the relay is transmitting
SDF-CDRT	Relay: one bit for indicating ε_1 or non-ε_1 event	One bit for indicating either x_b or x_r is transmitted
ISDF	U_1: one bit for indicating $\hat{\varepsilon}_1$ and $\hat{\varepsilon}_2$; U_2: two bits for indicating $\tilde{\varepsilon}_1$, $\tilde{\varepsilon}_2$, and $\tilde{\varepsilon}_3$	Two bits for indicating which one of $\{x_1, x_2, x_b\}$ is transmitted

received signal in the first time slot, which is characterized by

$$\gamma_{1,\mathrm{isdf}}^{x_1}(\varepsilon_1, \hat{\varepsilon}_1, \tilde{\varepsilon}_2) \geq \gamma_{\mathrm{th},1}. \tag{27}$$

At U_2, x_1 is detected based on the received signal in the first time slot. Since U_2 can detect x_1 successfully when $\tilde{\varepsilon}_2$ occurs, we have

$$\gamma_{2,\mathrm{isdf}}^{x_1}(\varepsilon_1, \hat{\varepsilon}_1, \tilde{\varepsilon}_2) \geq \gamma_{\mathrm{th},1}. \tag{28}$$

After subtracting the detected x_1 from the received signal of the first time slot, MRC is applied to the remaind signal and the received signal in the second time slot for recovering x_2. Thus, the end-to-end received SNR for detecting x_2 at U_2 is given by

$$\gamma_{2,\mathrm{isdf}}^{x_2}(\varepsilon_1, \hat{\varepsilon}_1, \tilde{\varepsilon}_2) = \rho(\alpha_2 |h_{s2}|^2 + |\tilde{h}_{r2}|^2). \tag{29}$$

B. Events $\{\varepsilon_1, \hat{\varepsilon}_1, \tilde{\varepsilon}_3\}$

When $\{\varepsilon_1, \hat{\varepsilon}_1, \tilde{\varepsilon}_3\}$ occurs, the relay forwards x_b in the second time slot. Since $\hat{\varepsilon}_1$ occurs in this case, U_1 detects x_1 based on the received signal in the first time slot. Thus, the end-to-end received SNR at U_1 for detecting x_1 satisfies

$$\gamma_{1,\mathrm{isdf}}^{x_1}(\varepsilon_1, \hat{\varepsilon}_1, \tilde{\varepsilon}_3) \geq \gamma_{\mathrm{th},1}. \tag{30}$$

At U_2, MRC is applied to detect x_1 based on the received signals from the two time slots. After then, SIC is performed for detecting x_2. The end-to-end received SNRs at U_2 for detecting x_1 and x_2 can be respectively expressed as

$$\gamma_{2,\mathrm{isdf}}^{x_1}(\varepsilon_1, \hat{\varepsilon}_1, \tilde{\varepsilon}_3) = \frac{\alpha_1 \rho(|h_{s2}|^2 + |\tilde{h}_{r2}|^2)}{\alpha_2 \rho(|h_{s2}|^2 + |\tilde{h}_{r2}|^2) + 1} \tag{31}$$

and

$$\gamma_{2,\mathrm{isdf}}^{x_2}(\varepsilon_1, \hat{\varepsilon}_1, \tilde{\varepsilon}_3) = \alpha_2 \rho(|h_{s2}|^2 + |\tilde{h}_{r2}|^2). \tag{32}$$

C. Events $\{\varepsilon_1, \hat{\varepsilon}_2, \tilde{\varepsilon}_1\}$

In this case, the relay forwards x_1 with its full transmit power to aid U_1. At U_1, MRC is applied for detecting x_1 with the end-to-end received SNR given by

$$\gamma_{1,\mathrm{isdf}}^{x_1}(\varepsilon_1, \hat{\varepsilon}_2, \tilde{\varepsilon}_1) = \frac{\rho(\alpha_1 |h_{s1}|^2 + |\tilde{h}_{r1}|^2)}{\alpha_2 \rho |h_{s1}|^2 + 1}. \tag{33}$$

Due to $\tilde{\varepsilon}_1$, U_2 detects its desired messages based on its received signal in the first time slot. The end-to-end received SNRs at U_2 satisfy

$$\gamma_{2,\mathrm{isdf}}^{x_1}(\varepsilon_1, \hat{\varepsilon}_2, \tilde{\varepsilon}_1) \geq \gamma_{\mathrm{th},1} \tag{34}$$

and

$$\gamma_{2,\mathrm{isdf}}^{x_2}(\varepsilon_1, \hat{\varepsilon}_2, \tilde{\varepsilon}_1) \geq \gamma_{\mathrm{th},2}. \tag{35}$$

D. Events $\{\varepsilon_1, \hat{\varepsilon}_2, \tilde{\varepsilon}_2\}$

When $\{\varepsilon_1, \hat{\varepsilon}_2, \tilde{\varepsilon}_2\}$ occurs, x_b is forwarded by the relay and MRC is applied at both users. The end-to-end received SNR at U_1 for detecting x_1 is given by

$$\gamma_{1,\mathrm{isdf}}^{x_1}(\varepsilon_1, \hat{\varepsilon}_2, \tilde{\varepsilon}_1) = \frac{\alpha_1 \rho(|h_{s1}|^2 + |\tilde{h}_{r1}|^2)}{\alpha_2 \rho(|h_{s1}|^2 + |\tilde{h}_{r1}|^2) + 1}. \tag{36}$$

Since that $\tilde{\varepsilon}_2$ already occurs in the first time slot, the end-to-end received SNR for U_2 to detect x_1 with the aid of MRC also satisfies

$$\gamma_{2,\mathrm{isdf}}^{x_1}(\varepsilon_1, \hat{\varepsilon}_2, \tilde{\varepsilon}_2) \geq \gamma_{\mathrm{th},1}. \tag{37}$$

Moreover, the end-to-end received SNR for U_2 to detect x_2 is the same as that of (32).

E. Events $\{\varepsilon_1, \hat{\varepsilon}_2, \tilde{\varepsilon}_3\}$

Since x_b is forwarded by the relay, the end-to-end received SNR at U_1 is the same as that of (36). At U_2, the end-to-end received SNRs for detecting x_1 and x_2 are the same as those of (31) and (32), respectively.

F. Events $\{\varepsilon_2, \hat{\varepsilon}_1, \tilde{\varepsilon}_3\}$

In this case, the relay can only forward x_1 taking into account ε_2. Due to the event $\hat{\varepsilon}_1$, we have $\gamma_{1,\mathrm{isdf}}^{x_1}(\varepsilon_2, \hat{\varepsilon}_1, \tilde{\varepsilon}_3) \geq \gamma_{\mathrm{th},1}$. At U_2, the end-to-end received SNRs for detecting x_1 and x_2 can be respectively derived as

$$\gamma_{2,\mathrm{isdf}}^{x_1}(\varepsilon_2, \hat{\varepsilon}_1, \tilde{\varepsilon}_3) = \frac{\rho(\alpha_1|h_{s2}|^2 + |\tilde{h}_{r2}|^2)}{\alpha_2\rho|h_{s2}|^2 + 1} \tag{38}$$

and

$$\gamma_{2,\mathrm{isdf}}^{x_2}(\varepsilon_2, \hat{\varepsilon}_1, \tilde{\varepsilon}_3) = \alpha_2\rho|h_{s2}|^2. \tag{39}$$

G. Events $\{\varepsilon_2, \hat{\varepsilon}_2, \tilde{\varepsilon}_1\}$

Only x_1 is forwarded in this case. The end-to-end received SNR at U_1 is the same as that of (33). Moreover, the end-to-end received SNRs at U_2 are characterized by $\gamma_{2,\mathrm{isdf}}^{x_1}(\varepsilon_2, \hat{\varepsilon}_2, \tilde{\varepsilon}_1) \geq \gamma_{\mathrm{th},1}$ and $\gamma_{2,\mathrm{isdf}}^{x_2}(\varepsilon_2, \hat{\varepsilon}_2, \tilde{\varepsilon}_1) \geq \gamma_{\mathrm{th},2}$.

H. Events $\{\varepsilon_2, \hat{\varepsilon}_2, \tilde{\varepsilon}_2\}$

In this case, the relay can forward only x_1 due to ε_2, so that the end-to-end received SNR at U_1 can be enhanced by using MRC as that of (33). At U_2, the end-to-end received SNRs are based on its received signal in the first time slot, which are characterized by $\gamma_{2,\mathrm{isdf}}^{x_1}(\varepsilon_2, \hat{\varepsilon}_2, \tilde{\varepsilon}_2) \geq \gamma_{\mathrm{th},1}$ and $\gamma_{2,\mathrm{isdf}}^{x_2}(\varepsilon_2, \hat{\varepsilon}_2, \tilde{\varepsilon}_2) < \gamma_{\mathrm{th},2}$.

I. Events $\{\varepsilon_2, \hat{\varepsilon}_2, \tilde{\varepsilon}_3\}$

In this case, the relay forwards x_1 with its full transmit power. Both U_1 and U_2 apply MRC to enhance the received SNRs. Thus, the end-to-end received SNR at U_1 for detecting x_1 has the same form as that of (33). At U_2, the end-to-end received SNRs for detecting x_1 and x_2 are the same as those of (38) and (39), respectively.

J. Events for Relay to Keep Silent

For all the scenarios in which the relay keeps silent regarding Table III, the end-to-end received SNRs at U_1 and U_2 are the same as those achieved by the direct link transmissions in the first time slot, which are characterized by the corresponding events $\{\hat{e}_j, \tilde{e}_k\}$.

It is worthwhile to point out that all the 18 combinations of the received SNR event $\{\varepsilon_i, \hat{\varepsilon}_j, \tilde{\varepsilon}_k\}$ belong to the above ten cases. Moreover, these events can be classified into three types, i.e., outage event, non-outage event, and undetermined event as summarized in Table VII in Appendix B, which will be used to facilitate the outage probability analysis for the ISDF scheme. For the proposed FR, SDF-CDRT, and ISDF schemes, the required feedback for the received SNR and control signaling for detection processing are summarized in Table IV. Especially, we can see that the required feedback and signaling for the FR and SDF-CDRF schemes are small and realistic. Although the received SNR events have 18 combinations in the ISDF scheme, the required control signaling at each receiver is still small, i.e., only the indicating information for the transmitted $\{x_1, x_2, x_b\}$ is needed for the SIC/MRC processing.

IV. Outage Probability Analyses

In this section, we perform the outage probability analyses for the FR, SDF-CDRT, and ISDF schemes, respectively. The closed-form expressions are derived for the outage probabilities achieved by the FR, SDF-CDRT, and ISDF schemes, respectively. Then, asymptotic outage performance analyses for the FR, SDF-CDRT, and ISDF schemes are respectively derived in the high transmit SNR region.

A. FR Scheme

For the conventional FR scheme, each receiver always combines the received signals from the two time slots for detecting its desired message irrespective of the decision results made at the relay. Accordingly, error propagation due to the incorrect detections at the relay cannot be avoided. With respect to the three types of the received SNR events at the relay, the outage probabilities achieved by the FR scheme at U_1 and U_2 can be respectively expressed as

$$P_{\mathrm{out},1}^{\mathrm{fr}} = \sum_{i=1}^{3} \Pr(\varepsilon_i)\mathcal{A}_1(\varepsilon_i) \tag{40}$$

and

$$P_{\mathrm{out},2}^{\mathrm{fr}} = \sum_{i=1}^{3} \Pr(\varepsilon_i)(\mathcal{A}_2(\varepsilon_i) + \mathcal{A}_3(\varepsilon_i)), \tag{41}$$

where $\mathcal{A}_1(\varepsilon_i) \triangleq \Pr\left\{\gamma_{1,\mathrm{fr}}^{x_1}(\varepsilon_i) < \gamma_{\mathrm{th},1}\right\}$, $\mathcal{A}_2(\varepsilon_i) \triangleq \Pr\left\{\gamma_{2,\mathrm{fr}}^{x_1}(\varepsilon_i) < \gamma_{\mathrm{th},1}\right\}$, and $\mathcal{A}_3(\varepsilon_i) \triangleq \Pr\left\{\gamma_{2,\mathrm{fr}}^{x_1}(\varepsilon_i) \geq \gamma_{\mathrm{th},1}, \gamma_{2,\mathrm{fr}}^{x_2}(\varepsilon_i) < \gamma_{\mathrm{th},2}\right\}$.

Since we assumed that all the channel gains follow i.n.i.d. exponential distributions, the probabilities of the received SNR events at the relay can be obtained as

$$\Pr\{\varepsilon_1\} = e^{-\frac{\xi_{\max}}{\beta_{sr}}}, \tag{42}$$

$$\Pr\{\varepsilon_2\} = \left[e^{-\frac{\xi_1}{\beta_{sr}}} - e^{-\frac{\xi_2}{\beta_{sr}}}\right]^+, \tag{43}$$

and

$$\Pr\{\varepsilon_3\} = 1 - e^{-\frac{\xi_1}{\beta_{sr}}}, \tag{44}$$

where $\xi_1 = \frac{\gamma_{\mathrm{th},1}}{\rho(\alpha_1 - \alpha_2\gamma_{\mathrm{th},1})}$, $\xi_2 = \frac{\gamma_{\mathrm{th},2}}{\alpha_2\rho}$, $\xi_{\max} \triangleq \max(\xi_1, \xi_2)$, and $[x]^+ \triangleq \max(x, 0)$. After some mathematical manipulations, the terms $\mathcal{A}_1$, $\mathcal{A}_2$, and $\mathcal{A}_3$ are derived in Table V, where $\tilde{\beta}_i \triangleq \chi\beta_i$ for $i = 1$ and 2. Based on the result in Table V and (42)-(44), the closed-form evaluations for the outage probabilities of U_1 and U_2 can be readily conducted via (40) and (41).

Theorem 1: For the FR scheme, as $\rho \to \infty$, asymptotic outage probabilities at U_1 and U_2 are respectively given by

$$P_{\mathrm{out},1}^{\mathrm{fr},\infty} = \frac{\xi_1}{\beta_{sr}} \frac{\chi\beta_{r1}\gamma_{\mathrm{th},1}}{\beta_{s1}(\alpha_1 - \alpha_2\gamma_{\mathrm{th},1}) + \chi\beta_{r1}\gamma_{\mathrm{th},1}} \tag{45}$$

and

$$P_{\mathrm{out},2}^{\mathrm{fr},\infty} = \frac{\xi_1}{\beta_{sr}} \frac{\chi\beta_{r2}\gamma_{\mathrm{th},1}}{\beta_{s2}(\alpha_1 - \alpha_2\gamma_{\mathrm{th},1}) + \chi\beta_{r2}\gamma_{\mathrm{th},1}} + \frac{[\xi_2 - \xi_1]^+}{\beta_{sr}} \frac{\chi\beta_{r2}\gamma_{\mathrm{th},2}}{\chi\beta_{r2}\gamma_{\mathrm{th},2} + \beta_{s2}}. \tag{46}$$

TABLE V
$\mathcal{A}_i$ FOR THE OUTAGE PROBABILITY EXPRESSION OF THE FR SCHEME

$$\mathcal{A}_1(\varepsilon_1)=\begin{cases}1+\frac{\beta_{s1}e^{-\frac{\xi_1}{\beta_{s1}}}}{\tilde{\beta}_{r1}-\beta_{s1}}-\frac{\tilde{\beta}_{r1}e^{-\frac{\xi_1}{\tilde{\beta}_{r1}}}}{\tilde{\beta}_{r1}-\beta_{s1}}, & \tilde{\beta}_{r1}\neq\beta_{s1}\\ 1-e^{-\frac{\xi_1}{\beta_{s1}}}\big(1+\frac{\xi_1}{\beta_{s1}}\big), & \tilde{\beta}_{r1}=\beta_{s1}\end{cases}$$

$$\mathcal{A}_1(\varepsilon_2)=\mathcal{A}_1(\varepsilon_1)$$

$$\mathcal{A}_1(\varepsilon_3)=1-\frac{\beta_{s1}e^{-\frac{\xi_1}{\beta_{s1}}}}{\rho\tilde{\beta}_{r1}\xi_1+\beta_{s1}}$$

$$\mathcal{A}_2(\varepsilon_1)=\begin{cases}1+\frac{\beta_{s2}e^{-\frac{\xi_1}{\beta_{s2}}}}{\tilde{\beta}_{r2}-\beta_{s2}}-\frac{\tilde{\beta}_{r2}e^{-\frac{\xi_1}{\tilde{\beta}_{r2}}}}{\tilde{\beta}_{r2}-\beta_{s2}}, & \tilde{\beta}_{r2}\neq\beta_{s2}\\ 1-e^{-\frac{\xi_1}{\beta_{s2}}}\big(1+\frac{\xi_1}{\beta_{s2}}\big), & \tilde{\beta}_{r2}=\beta_{s2}\end{cases}$$

$$\mathcal{A}_2(\varepsilon_2)=\mathcal{A}_2(\varepsilon_1)$$

$$\mathcal{A}_2(\varepsilon_3)=1-\frac{\beta_{s2}e^{-\frac{\xi_1}{\beta_{s2}}}}{\rho\tilde{\beta}_{r2}\xi_1+\beta_{s2}}$$

$$\mathcal{A}_3(\varepsilon_1)=\begin{cases}\left[\frac{\tilde{\beta}_{r2}\left(e^{-\frac{\xi_1}{\tilde{\beta}_{r2}}}-e^{-\frac{\xi_2}{\tilde{\beta}_{r2}}}\right)}{\tilde{\beta}_{r2}-\beta_{s2}}+\frac{\beta_{s2}\left(e^{-\frac{\xi_2}{\beta_{s2}}}-e^{-\frac{\xi_1}{\beta_{s2}}}\right)}{\tilde{\beta}_{r2}-\beta_{s2}}\right]^+, & \tilde{\beta}_{r2}\neq\beta_{s2}\\ \left[e^{-\frac{\xi_1}{\beta_{s2}}}\left(1+\frac{\xi_1}{\beta_{s2}}\right)-e^{-\frac{\xi_2}{\beta_{s2}}}\left(1+\frac{\xi_2}{\beta_{s2}}\right)\right]^+, & \tilde{\beta}_{r2}=\beta_{s2}\end{cases}$$

$$\mathcal{A}_3(\varepsilon_2)=\begin{cases}e^{-\frac{\xi_1}{\tilde{\beta}_{r2}}}+\frac{\beta_{s2}\left(e^{-\frac{\xi_1}{\tilde{\beta}_{r2}}}-e^{-\frac{\xi_1}{\beta_{s2}}}\right)}{\tilde{\beta}_{r2}-\beta_{s2}}-\frac{\beta_{s2}e^{-\frac{\xi_2}{\beta_{s2}}}}{\alpha_2\tilde{\beta}_{r2}\rho\xi_2+\beta_{s2}}, & \tilde{\beta}_{r2}\neq\beta_{s2},\xi_2>\xi_1\\ \frac{\tilde{\beta}_{r2}e^{-\frac{\xi_1}{\tilde{\beta}_{r2}}}}{\tilde{\beta}_{r2}-\beta_{s2}}-\frac{\tilde{\beta}_{r2}\beta_{s2}(1+\alpha_2\rho\xi_2)e^{-\frac{\xi_1(\alpha_2\tilde{\beta}_{r2}\rho\xi_2+\beta_{s2})+\xi_2(\tilde{\beta}_{r2}-\beta_{s2})}{\tilde{\beta}_{r2}\beta_{s2}(1+\alpha_2\rho\xi_2)}}}{(\tilde{\beta}_{r2}-\beta_{s2})(\alpha_2\tilde{\beta}_{r2}\rho\xi_2+\beta_{s2})}, & \tilde{\beta}_{r2}\neq\beta_{s2},\xi_2\leq\xi_1\\ \frac{(\beta_{s2}+\xi_1)e^{-\frac{\xi_1}{\beta_{s2}}}}{\beta_{s2}}-\frac{e^{-\frac{\xi_2}{\beta_{s2}}}}{1+\alpha_2\rho\xi_2}, & \tilde{\beta}_{r2}=\beta_{s2},\xi_2>\xi_1\\ \frac{\xi_2(1+\alpha_2\rho(\beta_{s2}+\xi_1))e^{-\frac{\xi_1}{\beta_{s2}}}}{\beta_{s2}(1+\alpha_2\rho\xi_2)}, & \tilde{\beta}_{r2}=\beta_{s2},\xi_2\leq\xi_1\end{cases}$$

$$\mathcal{A}_3(\varepsilon_3)=\frac{\beta_{s2}e^{-\frac{\xi_1}{\beta_{s2}}}}{\tilde{\beta}_{r2}\rho\xi_1+\beta_{s2}}-\frac{\beta_{s2}e^{-\frac{\xi_2}{\beta_{s2}}}}{\tilde{\beta}_{r2}\rho\xi_2+\beta_{s2}}$$

Proof: Applying the fact that $e^{-x}\to 1-x$ as $x\to 0$ to (42)-(44) and the terms in Table IV, the asymptotic expressions for (40) and (41) can be readily derived as (45) and (46), respectively. ∎

Defining the diversity order achieved by U_i by

$$d^i=-\lim_{\rho\to\infty}\frac{\log(P^{\mathrm{fr}}_{\mathrm{out},i})}{\log(\rho)} \tag{47}$$

and based on (45) and (46), it can be shown that both U_1 and U_2 achieve a diversity order of one when the FR scheme is applied. Considering that relaying occurs in each transmission block, the average throughput achieved by the FR scheme for U_i $(i=1,2)$ can be expressed as follows:

$$R^{\mathrm{fr}}_i=\frac{1}{2}R_i\big(1-P^{\mathrm{fr}}_{\mathrm{out},i}\big), \tag{48}$$

where the factor $\frac{1}{2}$ is resulted from half-duplex relaying.

B. SDF-CDRT Scheme

In the SDF-CDRT scheme, the operation at the relay depends on its own received SNR events, which also results in different end-to-end received SNRs at U_1 and U_2. Based on the derived end-to-end received SNRs at U_1 and U_2 and the received SNR events at the relay, the outage probabilities at U_1 and U_2 can be respectively expressed as

$$P^{\mathrm{sdf-cdrt}}_{\mathrm{out},1}=\sum_{i=1}^{3}\Pr\{\varepsilon_i\}\mathcal{B}_1(\varepsilon_i) \tag{49}$$

and

$$P^{\mathrm{sdf-cdft}}_{\mathrm{out},2}=\sum_{i=1}^{3}\Pr\{\varepsilon_i\}\mathcal{B}_2(\varepsilon_i), \tag{50}$$

where $\mathcal{B}_1(\varepsilon_i) \triangleq \Pr\{\gamma^{x_1}_{1,\mathrm{sdf-cdrt}}(\varepsilon_i) < \gamma_{\mathrm{th},1}\}$, $\mathcal{B}_2(\varepsilon_1) \triangleq \Pr\{\gamma^{x_2}_{2,\mathrm{sdf-cdrt}}(\varepsilon_1) < \gamma_{\mathrm{th},2}\}$, and $\mathcal{B}_2(\varepsilon_i) \triangleq \Pr\{\gamma^{x_1}_{2,\mathrm{sdf-cdrt}}(\varepsilon_i) < \gamma_{\mathrm{th},1}\} + \Pr\{\gamma^{x_1}_{2,\mathrm{sdf-cdrt}}(\varepsilon_i) \geq \gamma_{\mathrm{th},1}, \gamma^{x_2}_{2,\mathrm{idf}}(\varepsilon_i) < \gamma_{\mathrm{th},2}\}$ for $i = 2$ and 3. After some mathematical manipulations (see Appendix A), $\mathcal{B}_1$ and $\mathcal{B}_2$ are derived as follows:

$$\mathcal{B}_1(\varepsilon_1) = 1 - \frac{2\gamma_{\mathrm{th},1}}{\rho}\sqrt{\frac{\alpha_1\alpha_2}{\beta_{s1}\tilde{\beta}_{r1}}}e^{-\left(\frac{\alpha_2}{\beta_{r1}}+\frac{\alpha_1}{\beta_{s1}}\right)\frac{\gamma_{\mathrm{th},1}}{\rho}} \times K_1\left(\frac{2\gamma_{\mathrm{th},1}}{\rho}\sqrt{\frac{\alpha_1\alpha_2}{\beta_{s1}\tilde{\beta}_{r1}}}\right), \tag{51}$$

$$\mathcal{B}_1(\varepsilon_2) = \mathcal{B}_1(\varepsilon_3) = 1 - e^{-\frac{\xi_1}{\beta_{s1}}}, \tag{52}$$

$$\mathcal{B}_2(\varepsilon_1) = 1 - \frac{2\gamma_{\mathrm{th},2}}{\rho}\sqrt{\frac{\alpha_1\alpha_2}{\beta_{s2}\tilde{\beta}_{r2}}}e^{-\left(\frac{\alpha_2}{\beta_{r2}}+\frac{\alpha_1}{\beta_{s2}}\right)\frac{\gamma_{\mathrm{th},2}}{\rho}} \times K_1\left(\frac{2\gamma_{\mathrm{th},2}}{\rho}\sqrt{\frac{\alpha_1\alpha_2}{\beta_{s2}\tilde{\beta}_{r2}}}\right), \tag{53}$$

and

$$\mathcal{B}_2(\varepsilon_2) = \mathcal{B}_2(\varepsilon_3) = 1 - e^{-\frac{\xi_1}{\beta_{s2}}} + \left[e^{-\frac{\xi_1}{\beta_{s2}}} - e^{-\frac{\xi_2}{\beta_{s2}}}\right]^+. \tag{54}$$

Theorem 2: For the SDF-CDRT scheme, asymptotic outage probabilities at U_1 and U_2 are respectively given by

$$P^{\mathrm{sdf-cdrt},\infty}_{\mathrm{out},1} = \frac{\gamma_{\mathrm{th},1}}{\rho}\left(\frac{\alpha_2}{\chi\beta_{r1}} + \frac{\alpha_1}{\beta_{s1}}\right) + \frac{\xi_1([\xi_2 - \xi_1]^+ + \xi_1)}{\beta_{sr}\beta_{s1}} \tag{55}$$

and

$$P^{\mathrm{sdf-cdrt},\infty}_{\mathrm{out},2} = \frac{\gamma_{\mathrm{th},2}}{\rho}\left(\frac{\alpha_2}{\chi\beta_{r2}} + \frac{\alpha_1}{\beta_{s2}}\right) + \frac{([\xi_2 - \xi_1]^+ + \xi_1)^2}{\beta_{sr}\beta_{s2}}. \tag{56}$$

Proof: As $x \to 0$, applying the fact that $e^{-x} \to 1 - x$ and $xK_1(x) \to 1$ to (42)-(44) and $\mathcal{B}_1$ and $\mathcal{B}_2$, the asymptotic expressions for (49) and (50) can be readily derived as (55) and (56), respectively. ∎

With the obtained asymptotic expressions for the outage probabilities, it can be shown that both U_1 and U_2 achieve a diversity order of one when the SDF-CDRT scheme is applied. Since a relaying transmission occurs only when ε_1 happens in the SDF-CDRT scheme, whereas a new transmission block starts when ε_2 or ε_3 occurs, the average throughput achieved by the SDF-CDRT scheme for U_i $(i = 1, 2)$ can be expressed as follows:

$$R_i^{\mathrm{sdf-cdrt}} = \frac{1}{2}R_i\big(1 - \Pr\{\varepsilon_1\}\mathcal{B}_i(\varepsilon_1)\big) + R_i\left(1 - \sum_{k=2}^{3}\Pr\{\varepsilon_k\}\mathcal{B}_i(\varepsilon_k)\right). \tag{57}$$

C. ISDF Scheme

Since the relaying is switched on or off depending on not only the received SNR event feedback from two users, but also the received SNRs at the relay, the outage events at U_1 and U_2 occur regarding the combinations of $\{\varepsilon_i, \hat{\varepsilon}_j, \tilde{\varepsilon}_k\}$. Noting that non-outage events always occur when $\hat{\varepsilon}_1$ happens at U_1, the outage probability achieved by the ISDF scheme at U_1 can be expressed as

$$\begin{aligned} P^{\mathrm{isdf}}_{1,\mathrm{out}} &= \sum_{i=1}^{3}\sum_{k=1}^{3}\Pr\{\varepsilon_i\}\Pr\left\{\hat{\varepsilon}_2, \tilde{\varepsilon}_k, \gamma^{x_1}_{u_1,\mathrm{isdf}}(\varepsilon_i, \hat{\varepsilon}_j, \tilde{\varepsilon}_k) < \gamma_{\mathrm{th},1}\right\} \\ &= \sum_{i=1}^{3}\sum_{k=1}^{3}\Pr\{\varepsilon_i\}\Pr\{\tilde{\varepsilon}_k\}\Pr\left\{\hat{\varepsilon}_2, \gamma^{x_1}_{u_1,\mathrm{isdf}}(\varepsilon_i, \hat{\varepsilon}_j, \tilde{\varepsilon}_k) < \gamma_{\mathrm{th},1}\right\}. \end{aligned} \tag{58}$$

In (58), we have applied the fact that the event $\tilde{\varepsilon}_k$ is independent of $\hat{\varepsilon}_2$. Similarly, the outage probability at U_2 can be expressed as

$$\begin{aligned} P^{\mathrm{isdf}}_{2,\mathrm{out}} = \sum_{i=1}^{3}\sum_{j=1}^{2}\sum_{k=2}^{3}\Pr\{\varepsilon_i\}\Pr\{\hat{\varepsilon}_j\}\Pr\Big\{&\tilde{\varepsilon}_k, \gamma^{x_1}_{u_2,\mathrm{isdf}}(\varepsilon_i, \hat{\varepsilon}_j, \tilde{\varepsilon}_k) \\ &< \gamma_{\mathrm{th},1}\Big\} + \Pr\{\varepsilon_i\}\Pr\{\hat{\varepsilon}_j\}\Pr\Big\{\tilde{\varepsilon}_k, \gamma^{x_1}_{u_2,\mathrm{isdf}}(\varepsilon_i, \hat{\varepsilon}_j, \tilde{\varepsilon}_k) \\ &\geq \gamma_{\mathrm{th},1}, \gamma^{x_2}_{u_2,\mathrm{isdf}}(\varepsilon_i, \hat{\varepsilon}_j, \tilde{\varepsilon}_k) < \gamma_{\mathrm{th},2}\Big\}. \end{aligned} \tag{59}$$

In (58) and (59), the probabilities $\Pr\{\hat{\varepsilon}_j\}$ and $\Pr\{\hat{\varepsilon}_k\}$ can be derived as

$$\Pr\{\hat{\varepsilon}_1\} = e^{-\frac{\xi_1}{\beta_{s1}}}, \tag{60}$$

$$\Pr\{\hat{\varepsilon}_2\} = 1 - e^{-\frac{\xi_1}{\beta_{s1}}}, \tag{61}$$

$$\Pr\{\tilde{\varepsilon}_1\} = e^{-\frac{\xi_{\max}}{\beta_{s2}}}, \tag{62}$$

$$\Pr\{\tilde{\varepsilon}_2\} = \left[e^{-\frac{\xi_1}{\beta_{s2}}} - e^{-\frac{\xi_2}{\beta_{s2}}}\right]^+, \tag{63}$$

and

$$\Pr\{\tilde{\varepsilon}_3\} = 1 - e^{-\frac{\xi_1}{\beta_{s2}}}. \tag{64}$$

Theorem 3: For the ISDF scheme, the achieved outage probabilities at U_1 and U_2 are respectively given by

$$P^{\mathrm{isdf}}_{\mathrm{out},1} = \widehat{\mathcal{P}}_1\big(\Pr\{\varepsilon_1\}\Pr\{\tilde{\varepsilon}_1\} + \Pr\{\varepsilon_2\}\big) + \widehat{\mathcal{P}}_2\Pr\{\varepsilon_1\} \times\big(1 - \Pr\{\tilde{\varepsilon}_1\}\big) + \Pr\{\varepsilon_3\}\Pr\{\hat{\varepsilon}_2\} \tag{65}$$

and

$$\begin{aligned} P^{\mathrm{isdf}}_{\mathrm{out},2} = {}& \widetilde{\mathcal{P}}_1\Pr\{\varepsilon_1\}\Pr\{\hat{\varepsilon}_1\} + \widetilde{\mathcal{P}}_2\Pr\{\varepsilon_1\} \\ &+ \widetilde{\mathcal{P}}_3\Pr\{\varepsilon_1\}\Pr\{\hat{\varepsilon}_2\} + \widetilde{\mathcal{P}}_4\Pr\{\varepsilon_2\} \\ &+ \Pr\{\varepsilon_2\}\Pr\{\tilde{\varepsilon}_2\} + \Pr\{\varepsilon_3\}(1 - \Pr\{\tilde{\varepsilon}_1\}), \end{aligned} \tag{66}$$

where $\widehat{\mathcal{P}}_i$ $(i = 1, 2)$ and $\widetilde{\mathcal{P}}_j$ $(j = 1, 2, 3, 4)$ are given in Table VI.

Proof: See Appendix B. ∎

The expressions in Theorem 3 show that the outage probability at each user consists of two parts, i.e., one part due to the *Undetermined* SNR events and another part due to the *Outage* SNR events, as marked in Table VII in Appendix B. When $\rho \to \infty$, the *Undetermined* SNR events in Table VII tend to be non-outage. Thus, asymptotic expressions for the outage probabilities are mainly determined by the asymptotic values of the part corresponding to the *Outage* SNR events, which are respectively provided as

$$P^{\mathrm{isdf},\infty}_{\mathrm{out},1} = \frac{\xi_1^2}{\beta_{sr}\beta_{s1}} \tag{67}$$

TABLE VI

$\widehat{\mathcal{P}}_i$ AND $\widetilde{\mathcal{P}}_j$ FOR THE OUTAGE PROBABILITY EXPRESSIONS OF THE ISDF SCHEME

$$\widehat{\mathcal{P}}_1 = \begin{cases} \frac{\beta_{s1}\gamma_{\mathrm{th},1}\left(1-e^{-\frac{\xi_1}{\beta_{s1}}}\right)-\tilde{\beta}_{r1}\rho\xi_1\left(1-e^{-\frac{\gamma_{\mathrm{th},1}}{\tilde{\beta}_{r1}\rho}}\right)}{\beta_{s1}\gamma_{\mathrm{th},1}-\tilde{\beta}_{r1}\rho\xi_1}, & \beta_{s1} \neq \frac{\rho\tilde{\beta}_{r1}\xi_1}{\gamma_{\mathrm{th},1}} \\ 1-e^{-\frac{\xi_1}{\beta_{s1}}}\left(1+\frac{\xi_1}{\beta_{s1}}\right), & \beta_{s1} = \frac{\rho\tilde{\beta}_{r1}\xi_1}{\gamma_{\mathrm{th},1}} \end{cases}$$

$$\widehat{\mathcal{P}}_2 = \begin{cases} \frac{\tilde{\beta}_{r1}\left(1-e^{-\frac{\xi_1}{\tilde{\beta}_{r1}}}\right)-\beta_{s1}\left(1-e^{-\frac{\xi_1}{\beta_{s1}}}\right)}{\tilde{\beta}_{r1}-\beta_{s1}}, & \beta_{s1} \neq \tilde{\beta}_{r1} \\ 1-e^{-\frac{\xi_1}{\beta_{s1}}}\left(1+\frac{\xi_1}{\beta_{s1}}\right), & \beta_{s1} = \tilde{\beta}_{r1}. \end{cases}$$

$$\widetilde{\mathcal{P}}_1 = \begin{cases} \frac{\tilde{\beta}_{r2}e^{-\frac{\xi_1}{\beta_{s2}}}\left(1-e^{\frac{\alpha_2(\xi_1-\xi_2)}{\tilde{\beta}_{r2}}}\right)}{\tilde{\beta}_{r2}-\alpha_2\beta_{s2}} - \frac{\alpha_2\beta_{s2}\left(e^{-\frac{\xi_1}{\beta_{s2}}}-e^{-\frac{\xi_2}{\beta_{s2}}}\right)}{\tilde{\beta}_{r2}-\alpha_2\beta_{s2}}, & \tilde{\beta}_{r2} \neq \alpha_2\beta_{s2} \\ e^{-\frac{\xi_1}{\beta_{s2}}}-e^{-\frac{\xi_2}{\beta_{s2}}}\left(1+\frac{\xi_2-\xi_1}{\beta_{s2}}\right), & \tilde{\beta}_{r2} = \alpha_2\beta_{s2}, \end{cases}$$

$$\widetilde{\mathcal{P}}_2 = \begin{cases} 1-e^{-\frac{\xi_1}{\tilde{\beta}_{r2}}}+\frac{\beta_{s2}e^{-\frac{\xi_1}{\beta_{s2}}}\left(1-e^{\frac{\xi_1}{\beta_{s2}}-\frac{\xi_1}{\tilde{\beta}_{r2}}}\right)}{\tilde{\beta}_{r2}-\beta_{s2}}+\frac{\tilde{\beta}_{r2}\left(e^{\frac{\xi_1}{\tilde{\beta}_{r2}}-\frac{\xi_2}{\tilde{\beta}_{r2}}-\frac{\xi_1}{\beta_{s2}}}+e^{-\frac{\xi_1}{\tilde{\beta}_{r2}}}-e^{-\frac{\xi_2}{\tilde{\beta}_{r2}}}-e^{-\frac{\xi_1}{\beta_{s2}}}\right)}{\tilde{\beta}_{r2}-\beta_{s2}}, & \tilde{\beta}_{r2} \neq \beta_{s2} \\ 1-e^{-\frac{\xi_1}{\beta_{s2}}}-\frac{\xi_1}{\beta_{s2}}e^{-\frac{\xi_2}{\beta_{s2}}}, & \tilde{\beta}_{r2} = \beta_{s2}, \end{cases}$$

$$\widetilde{\mathcal{P}}_3 = \begin{cases} e^{-\frac{\xi_1}{\beta_{s2}}}+\frac{\beta_{s2}e^{-\frac{\xi_2}{\beta_{s2}}}}{\tilde{\beta}_{r2}-\beta_{s2}}-\frac{\tilde{\beta}_{r2}e^{\frac{\xi_1}{\tilde{\beta}_{r2}}-\frac{\xi_2}{\tilde{\beta}_{r2}}-\frac{\xi_1}{\beta_{s2}}}}{\tilde{\beta}_{r2}-\beta_{s2}}, & \tilde{\beta}_{r2} \neq \beta_{s2} \\ e^{-\frac{\xi_1}{\beta_{s2}}}-e^{-\frac{\xi_2}{\beta_{s2}}}\left(1+\frac{\xi_2-\xi_1}{\beta_{s2}}\right), & \tilde{\beta}_{r2} = \beta_{s2}, \end{cases}$$

$$\widetilde{\mathcal{P}}_4 = 1-e^{-\frac{\xi_1}{\beta_{s2}}}$$

and

$$P_{\mathrm{out},2}^{\mathrm{isdf},\infty} = \begin{cases} \frac{[\xi_2-\xi_1]^+([\xi_2-\xi_1]^++\xi_1)}{\beta_{sr}\beta_{s2}}+\frac{\xi_1(\xi_2-\xi_1)}{\chi\beta_{s2}\beta_{r2}}, & \chi\beta_{r2} \neq \beta_{s2} \\ \frac{[\xi_2-\xi_1]^+([\xi_2-\xi_1]^++\xi_1)}{\beta_{sr}\beta_{s2}}+\frac{\xi_1\xi_2}{\beta_{s2}^2}, & \chi\beta_{r2} = \beta_{s2}. \end{cases} \tag{68}$$

Based on (67), it can be seen that U_1 achieves a diversity order of two. As such, when $\xi_2 > \xi_1$, it can be seen that U_2 also achieves a diversity order of two. Compared to the FR and SDF-CDRT schemes, the ISDF scheme achieves a greater diversity order for both users.

In the ISDF scheme, a relaying transmission does not occur when $\{\hat{\varepsilon}_1, \tilde{\varepsilon}_1\}$ happens. In such a subcase, the corresponding average throughput achieved at U_1 is given by $R_1 \Pr\{\hat{\varepsilon}_1\}\Pr\{\tilde{\varepsilon}_1\}$. Moreover, an additional relaying transmission actually occurs only when either ε_1 or ε_2 happens according to Table III, whereas a new transmission block starts when ε_3 happens. In such a subcase, the corresponding outage probability is the first two terms on the righthand side of (65). Therefore, the average throughput achieved by the ISDF scheme for U_1 can be expressed as follows:

$$\begin{aligned} R_1^{\mathrm{isdf}} = {} & R_1 \Pr\{\hat{\varepsilon}_1\}\Pr\{\tilde{\varepsilon}_1\} + \frac{1}{2}R_1\big(1-\Pr\{\hat{\varepsilon}_1\}\Pr\{\tilde{\varepsilon}_1\}\big) \\ & \times\Big(1-\widehat{\mathcal{P}}_1\big(\Pr\{\varepsilon_1\}\Pr\{\tilde{\varepsilon}_1\}+\Pr\{\varepsilon_2\}\big) \\ & -\widehat{\mathcal{P}}_2\Pr\{\varepsilon_1\}\big(1-\Pr\{\tilde{\varepsilon}_1\}\big)\Big). \end{aligned} \tag{69}$$

As such, the average throughput achieved by the ISDF scheme for U_2 is given by

$$\begin{aligned} R_1^{\mathrm{isdf}} = {} & R_2 \Pr\{\hat{\varepsilon}_1\}\Pr\{\tilde{\varepsilon}_1\} + \frac{1}{2}R_2\big(1-\Pr\{\hat{\varepsilon}_1\}\Pr\{\tilde{\varepsilon}_1\}\big) \\ & \times\Big(1-\widetilde{\mathcal{P}}_1\Pr\{\varepsilon_1\}\Pr\{\hat{\varepsilon}_1\}-\widetilde{\mathcal{P}}_2\Pr\{\varepsilon_1\}-\widetilde{\mathcal{P}}_3 \\ & \Pr\{\varepsilon_1\}\Pr\{\hat{\varepsilon}_2\}-\widetilde{\mathcal{P}}_4\Pr\{\varepsilon_2\}-\Pr\{\varepsilon_2\}\Pr\{\tilde{\varepsilon}_2\}\Big). \end{aligned} \tag{70}$$

V. SIMULATION RESULTS

This section provides Monte Carlo simulation results to verify the correctness of the analytical results and evaluate the outage performance achieved by the proposed schemes. In the figures for the simulation results, the curves corresponding to the conventional FR schemes are denoted by "FR, Conv." and the curves corresponding to the DF relaying without direct links are denoted by "DF w/o DL". For simplicity, we set

TABLE VII
RECEIVED SNR EVENTS IN THE ISDF SCHEME

	$\{\hat{\varepsilon}_1, \tilde{\varepsilon}_1\}$		$\{\hat{\varepsilon}_1, \tilde{\varepsilon}_2\}$		$\{\hat{\varepsilon}_1, \tilde{\varepsilon}_3\}$	
	U_1	U_2	U_1	U_2	U_1	U_2
ε_1	$\gamma_{1,\text{isdf}}^{x_1} \geq \gamma_{\text{th},1}$	$\gamma_{2,\text{isdf}}^{x_1} \geq \gamma_{\text{th},1}$ $\gamma_{2,\text{isdf}}^{x_2} \geq \gamma_{\text{th},2}$	$\gamma_{1,\text{isdf}}^{x_1} \geq \gamma_{\text{th},1}$	$\gamma_{2,\text{isdf}}^{x_1} \geq \gamma_{\text{th},1}$ $\gamma_{2,\text{isdf}}^{x_2} = (29)$	$\gamma_{1,\text{isdf}}^{x_1} \geq \gamma_{\text{th},1}$	$\gamma_{2,\text{isdf}}^{x_1} = (31)$ $\gamma_{2,\text{isdf}}^{x_2} = (32)$
ε_2	$\gamma_{1,\text{isdf}}^{x_1} \geq \gamma_{\text{th},1}$	$\gamma_{2,\text{isdf}}^{x_1} \geq \gamma_{\text{th},1}$ $\gamma_{2,\text{isdf}}^{x_1 2} \geq \gamma_{\text{th},2}$	$\gamma_{1,\text{isdf}}^{x_1} \geq \gamma_{\text{th},1}$	$\gamma_{2,\text{isdf}}^{x_1} \geq \gamma_{\text{th},1}$ $\gamma_{2,\text{isdf}}^{x_2} < \gamma_{\text{th},2}$	$\gamma_{1,\text{isdf}}^{x_1} \geq \gamma_{\text{th},1}$	$\gamma_{2,\text{isdf}}^{x_1} = (38)$ $\gamma_{2,\text{isdf}}^{x_2} = (39)$
ε_3	$\gamma_{1,\text{isdf}}^{x_1} \geq \gamma_{\text{th},1}$	$\gamma_{2,\text{isdf}}^{x_1} \geq \gamma_{\text{th},1}$ $\gamma_{2,\text{isdf}}^{x_2} \geq \gamma_{\text{th},2}$	$\gamma_{1,\text{isdf}}^{x_1} \geq \gamma_{\text{th},1}$	$\gamma_{2,\text{isdf}}^{x_1} \geq \gamma_{\text{th},1}$ $\gamma_{2,\text{isdf}}^{x_2} < \gamma_{\text{th},2}$	$\gamma_{1,\text{isdf}}^{x_1} \geq \gamma_{\text{th},1}$	$\gamma_{2,\text{isdf}}^{x_1} < \gamma_{\text{th},1}$
	$\{\hat{\varepsilon}_2, \tilde{\varepsilon}_1\}$		$\{\hat{\varepsilon}_2, \tilde{\varepsilon}_2\}$		$\{\hat{\varepsilon}_2, \tilde{\varepsilon}_3\}$	
	U_1	U_2	U_1	U_2	U_1	U_2
ε_1	$\gamma_{1,\text{isdf}}^{x_1} = (33)$	$\gamma_{2,\text{isdf}}^{x_1} \geq \gamma_{\text{th},1}$ $\gamma_{2,\text{isdf}}^{x_2} \geq \gamma_{\text{th},2}$	$\gamma_{1,\text{isdf}}^{x_1} = (36)$	$\gamma_{2,\text{isdf}}^{x_1} \geq \gamma_{\text{th},1}$ $\gamma_{2,\text{isdf}}^{x_2} = (32)$	$\gamma_{1,\text{isdf}}^{x_1} = (36)$	$\gamma_{2,\text{isdf}}^{x_1} = (31)$ $\gamma_{2,\text{isdf}}^{x_1 2} = (32)$
ε_2	$\gamma_{1,\text{isdf}}^{x_1} = (33)$	$\gamma_{2,\text{isdf}}^{x_1} \geq \gamma_{\text{th},1}$ $\gamma_{2,\text{isdf}}^{x_2} \geq \gamma_{\text{th},2}$	$\gamma_{1,\text{isdf}}^{x_1} = (33)$	$\gamma_{2,\text{isdf}}^{x_1} \geq \gamma_{\text{th},1}$ $\gamma_{2,\text{isdf}}^{x_2} < \gamma_{\text{th},2}$	$\gamma_{1,\text{isdf}}^{x_1} = (33)$	$\gamma_{2,\text{isdf}}^{x_1} = (38)$ $\gamma_{2,\text{isdf}}^{x_2} = (39)$
ε_3	$\gamma_{1,\text{isdf}}^{x_1} < \gamma_{\text{th},1}$	$\gamma_{2,\text{isdf}}^{x_1} \geq \gamma_{\text{th},1}$ $\gamma_{2,\text{isdf}}^{x_2} \geq \gamma_{\text{th},2}$	$\gamma_{1,\text{isdf}}^{x_1} < \gamma_{\text{th},1}$	$\gamma_{2,\text{isdf}}^{x_1} \geq \gamma_{\text{th},1}$ $\gamma_{2,\text{isdf}}^{x_2} < \gamma_{\text{th},2}$	$\gamma_{1,\text{isdf}}^{x_1} < \gamma_{\text{th},1}$	$\gamma_{1,\text{isdf}}^{x_1} < \gamma_{\text{th},1}$

U_1: Non-outage Outage Undetermined

U_2: Non-outage Outage Undetermined

$\chi = 1$ assuming equal power allocation at the source and the relay.

The outage probability versus the transmit SNR is investigated in Fig. 2, where we consider two scenarios. For scenario 1, we set $\beta_{s1} = \beta_{s2} = 0.8$, and the remained $\beta_{ij} = 1$. For scenario 2, we set all $\beta_{ij} = 1$. The power allocation coefficient is set as $\alpha_1 = 0.8$ for both scenarios. In Fig. 2(a) and Fig. 2(b), the correctness of the analytical outage probability is verified by simulation results. The correctness of the asymptotic expressions for all the considered schemes is also verified in Fig. 2(a). It is shown that the ISDF scheme achieves the smallest outage probabilities for U_1 and U_2, respectively, in the whole SNR region. The SDF-CDRT scheme also achieves the smaller outage probabilities for U_1 and U_2 over those of the conventional FR scheme, respectively. In Fig. 2(a), at the 10^{-2} outage probability level, the ISDF and SDF-CDRT schemes respectively achieve about 9 dB and 4 dB SNR gains over that of the conventional FR scheme for U_1. The similar results can be observed for U_2 at the 10^{-2} outage probability level. Thus, the superior outage performance of the ISDF scheme is verified by Fig. 2. By applying selective relaying, the SDF-CDRT scheme not only prevents error propagation compared to the conventional FR scheme, but also avoids SIC when the BS-to-relay link is good enough (when ε_1 occurs). Due to error propagation at the relay, the conventional FR scheme achieves the highest outage probability in Fig. 2(a) and Fig. 2(b).

In Fig. 3, we investigate the impact of the target rate on the outage probability, where we set $\rho = 30$ dB and $\alpha_1 = 0.8$. In Fig. 3(a), we fix $R_1 = 2$ bps/Hz and increase R_2 from 2 to 10 bps/Hz. As it is shown in Fig. 3(a), the SDF-CDRT and ISDF scheme achieve the smaller outage probabilities than those of the conventional FR scheme for U_1 and U_2, respectively. For all the considered relaying schemes, the outage probability of U_2 increases by increasing R_2 and approaches one in the high target rate region. Also, the outage probability of U_1 achieved by the SDF-CDRT scheme increases by increasing R_2. In contrast, the outage probability of U_1 achieved by the conventional FR scheme keeps constant irrespective of the variation of R_2, while the outage probability of U_1 achieved by the ISDF scheme almost keeps constant by increasing R_2. In Fig. 3(b), we set $R_1 = 0.4\ R_2$ and investigate the impact of the target rate on the outage performance for different schemes. Note that when both R_1 and R_2 increase, the affordable outage performances of the different schemes can be observed. For U_1 and U_2, Fig. 3(b) shows that the outage probabilities achieved by all the schemes first increase by increasing the target rate and then jump to one as the target rate reaches a large value. It is shown that the ISDF scheme achieves the smallest outage probabilities for U_1 and U_2, respectively. The SDF-CDRT scheme also achieves the smaller outage probability for U_1 than that of the conventional FR scheme. However, for U_2, the SDF-CDRT scheme achieves the higher outage probability than that of the conventional FR scheme in the low target region. In the middle and high target rate regions, the SDF-CDRT scheme achieves the smaller outage probability than that of the conventional FR scheme, which is preferred by a higher QoS requirement.

To see the details of the impact of the power allocation on the outage performance, we investigate the outage probability

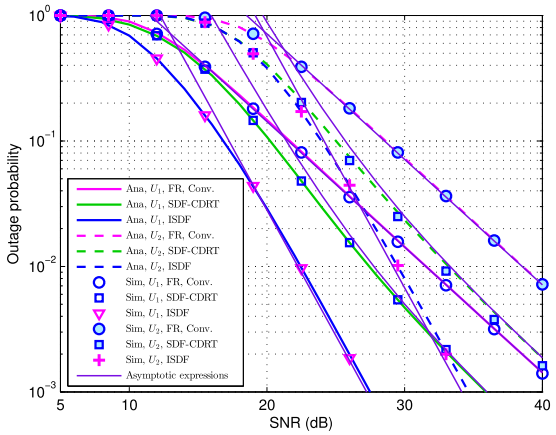

(a) Scenario 1 ($R_1 = 2$ bps/Hz, $R_2 = 4$ bps/Hz).

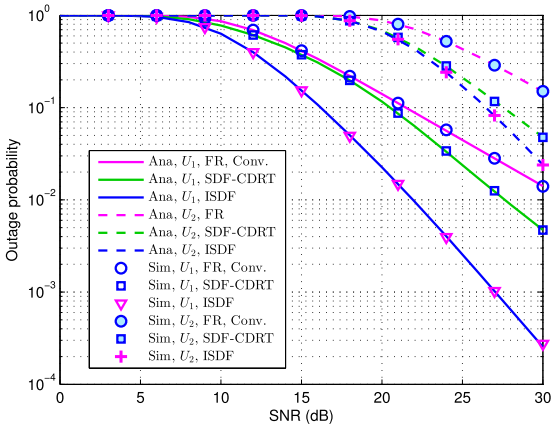

(b) Scenario 2 ($R_1 = 2$ bps/Hz, $R_2 = 5$ bps/Hz).

Fig. 2. Outage probability versus SNR.

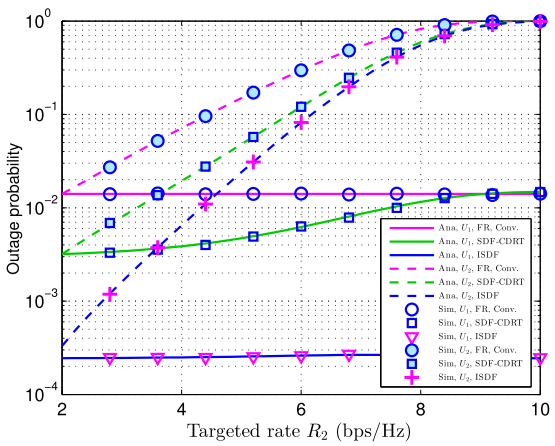

(a) Fixed $R_1 = 2$ bps/Hz in scenario 1.

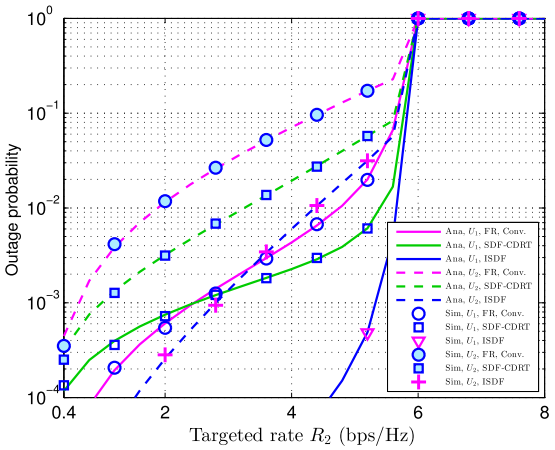

(b) $R_1 = 0.4R_2$ in scenario 2.

Fig. 3. Outage probability versus target rate.

versus α_1 in Fig. 4, where we set $\rho = 30$ dB, $R_1 = 2$ bps/Hz, and $R_2 = 5$ bps/Hz in scenario 2. It is shown in Fig. 4 that the ISDF scheme achieves the smallest outage probabilities for U_1 and U_2 in the whole α_1 region. For U_2, the SDF-CDRT scheme achieves the smaller outage probability than that of the conventional FR scheme. However, for U_1, the conventional FR scheme achieves the smaller outage probability than that of the SDF-CDRT scheme in the high α_1 region.

To investigate the impact of the relay's location on the outage performance, we also consider a geometric location model as depicted in Fig. 5(a), in which the BS is located at the center of a unit circle and two far users (U_1 and U_2) are located on the edge of the circle. For the comparison with the MUST scheme, we assume that two near users (U_3 and U_4) are located near the BS. In the geometric location model, we set the path loss model by $\beta_{ij} = d_{ij}^{-\tau}$, where the path loss exponent is set as $\tau = 3$ and d_{ij} is the distance between $i \in \{s, r\}$ and $j \in \{r, 1, 2, 3, 4\}$. For the simulation results in Fig. 5(b), we set $\rho = 30$ dB, $R_1 = 2$ bps/Hz, $R_2 = 5$ bps/Hz, $\theta_1 = 15°$, and $\theta_2 = -15°$. In the simulation, the relay moves away from the BS along the vertical direction. For the comparison purpose, the outage probabilities at U_1 and U_2 achieved by the DF relay without direct links and the direct link transmission using the MUST scheme (U_1 and U_2 are paired in terms of their target

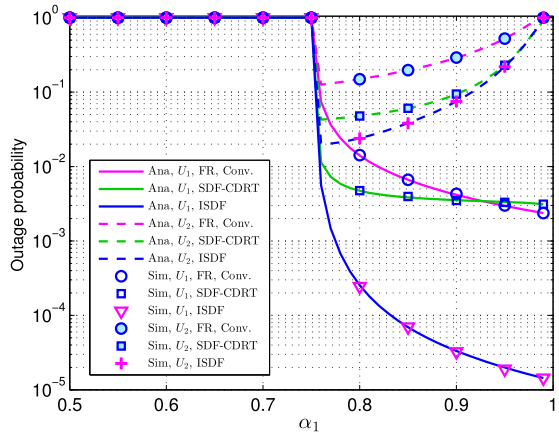

Fig. 4. Outage probability versus power allocation coefficient.

transmission rates) are also presented. It is shown that the ISDF scheme achieves the smallest outage probabilities for U_1 and U_2, respectively. As the distance d_{sr} increases from 0 to 0.9, the outage probabilities achieved by the ISDF scheme first decreases and then increases. Moreover, as d_{sr} approaches zero, the ISDF scheme becomes the MUST scheme with the retransmission protocol, which is described in Table II.

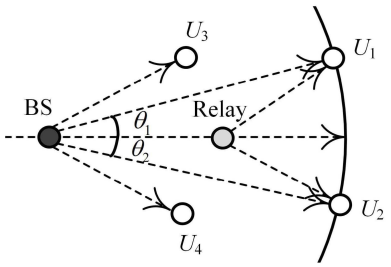

(a) The geometric location model.

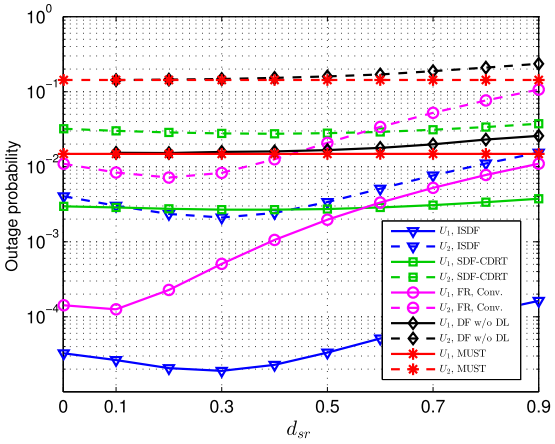

(b) Outage probability versus relay location.

Fig. 5. The impact of the relay location on the outage probability.

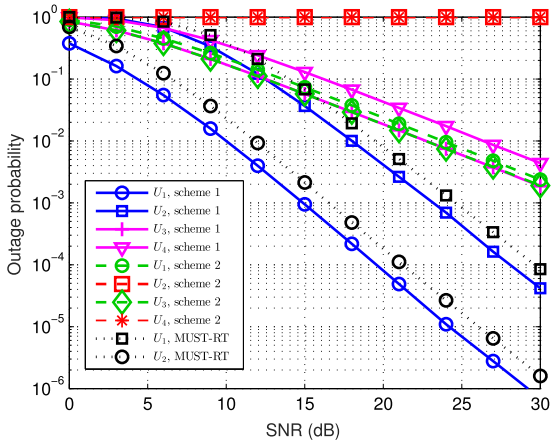

(a) Outage probability versus SNR.

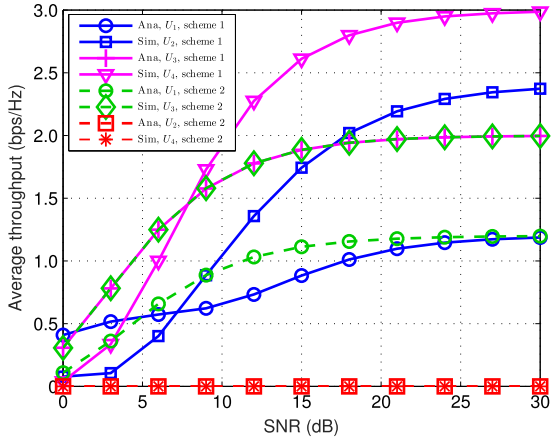

(b) Average throughput versus SNR.

Fig. 6. Performance comparison between the ISDF and MUST schemes.

However, this figure shows that the optimal location of the relay is not $d_{sr} = 0$, so that the ISDF scheme can effectively decrease the outage probability even compared with MUST with the retransmission protocol. In the small and middle d_{sr} regions, it is shown that the conventional FR scheme achieves the smaller outage probabilities than those of the SDF-CDRT scheme for U_1 and U_2, respectively. However, when the relay is located more close to the users, the SDF-CDRT scheme achieves the smaller outage probabilities than those of the conventional FR scheme for U_1 and U_2, respectively. For the SDF-CDRT scheme, the achieved outage probability at U_1 increases by increasing d_{sr}, whereas the achieved outage probability at U_2 first decreases and then increases by increasing d_{sr}. For the SDF-CDRT scheme, the achieved outage probabilities also first decrease and then increase by increasing d_{sr}. However, the variations are not dramatic compared to those of the ISDF and SDF-CDRT schemes. Moreover, all the considered schemes with direct links achieve the better outage performance over those of the "DF w/o DL" and MUST for the paired U_1 and U_2.

Considering the MUST scheme that pairs a far user and a near user in terms of their channel qualities, we compare the outage probability achieved by the proposed ISDF and MUST schemes in Fig. 6. The target transmission rates for U_1, U_2, U_3, and U_4 are set as 1.2 bps/Hz, 2.4 bps/Hz, 2 bps/Hz, and 3 bps/Hz, respectively. The distances from the BS to the two near users (U_3 and U_4) are set by $d_{s3} = d_{s4} = 0.5$, as depicted in Fig. 5(a). The relay is located by $d_{sr} = 0.3$ referring to the results in Fig. 5(b). We assume that channel quality based pairing and QoS requirement based pairing are applied in scheme 1 and scheme 2, respectively. That is, in scheme 1, U_1 and U_2 are paired and the ISDF is deployed with the aid of the relay; U_3 and U_4 are paired in terms of their target transmission rates. In contrast, MUST is adopted in scheme 2, i.e., the far user U_1 is paired with the near user U_3, meanwhile U_2 is paired with U_4. For the two users in each pair, we assume that $\alpha_1 = 0.8$ and $\alpha_2 = 0.2$ are applied for the power allocation.

It is shown in Fig. 6(a) that scheme 1 achieves lower outage probabilities for U_1, U_2, and U_4 than those of scheme 2. Only for U_3 do the two schemes achieve the same outage probabilities. When scheme 2 is applied, the outage probabilities of both U_2 and U_4 are both equal to one, which indicates that MUST cannot support a higher rate transmission for the paired U_2 and U_4. However, scheme 1 achieves a lower outage probability for U_2 than those of U_3 and U_4 in the middle and high SNR regions, even if the far user U_2 has a relatively higher target transmission rate. Note that scheme 1 degenerates to MUST with retransmission (MUST-RT) when $d_{sr} = 0$ regarding Table II. The outage probabilities achieved by MUST-RT for

the paired U_1 and U_2 are also presented in Fig. 6(a). It is shown that MUST-RT achieves larger outage probabilities for the paired U_1 and U_2 than those of scheme 1. Under the same simulation parameters, the average throughputs achieved by scheme 1 and scheme 2 are plotted in Fig. 6(b). The results in Fig. 6(b) clearly show that scheme 1 achieves non-zero average throughputs for all the users in the whole SNR region, whereas scheme 2 achieves zero throughputs for the paired U_2 and U_4. For the far user U_2 with a relatively higher target transmission rate, scheme 1 achieves a remarkable average throughput in the whole SNR region. The similar results are also observed for U_4. Although scheme 2 achieves a larger average throughput for U_1 in the middle SNR region than scheme 1, obviously scheme 1 achieves a much larger sum rate than scheme 2. Therefore, the proposed ISDF scheme provides better rate performance than the MUST scheme, especially when the far user has demanding QoS requirements.

VI. Conclusions

In this paper, we have investigated the FR, SDF-CDRT, and ISDF schemes for the cooperative NOMA system with non-negligible direct links from the BS to two far users. To reduce error propagation resulted from the incorrect detections at the relay, the SDF-CDRT and ISDF schemes take into account the received SNRs at the relay and operate in the DF mode adaptively. When the relay can detect its received signal correctly, the SDF-CDRT can avoid SIC at the receiver side by forming an orthogonal transmission branch with respect to the direct link. For the ISDF scheme, unnecessary relaying can be reduced by exploiting the limited feedback of the received SNR events from the two users. For the considered three cooperative relaying schemes, the outage probabilities have been derived in closed-form for the two users along with the asymptotic expressions for the outage probabilities and diversity orders. Simulation results have verified the superior outage performance achieved by the proposed cooperative relaying schemes over those of the cooperative DF relaying without direct links and MUST without relaying.

Appendix A
A Derivation for $\mathcal{B}_1$ and $\mathcal{B}_1$

In this part, we evaluate the terms $\mathcal{B}_1$ and $\mathcal{B}_2$. The term $\mathcal{B}_1(\varepsilon_1)$ can be rewritten as

$$\mathcal{B}_1(\varepsilon_1) = \Pr\left\{Y < \frac{2\alpha_1\alpha_2\gamma_{\text{th},1}}{\rho}\right\}, \tag{A.1}$$

where the RV Y is defined as

$$Y \triangleq \frac{2Y_1Y_2}{Y_1+Y_2} \tag{A.2}$$

with $Y_1 \triangleq \alpha_2|h_{s1}|^2$ and $Y_2 \triangleq \alpha_1|h_{r1}|^2$ following i.n.i.d. exponential distributions. Since that Y is the harmonic mean of two i.n.i.d exponential RVs, the cumulative distribution function (CDF) of Y can be expressed as [42]

$$F_Y(y) = 1 - \frac{y}{\sqrt{\alpha_1\alpha_2\beta_{s1}\tilde{\beta}_{r1}}} e^{-\frac{y}{2}\left(\frac{1}{\alpha_2\tilde{\beta}_{r1}}+\frac{1}{\alpha_1\beta_{s1}}\right)} \times K_1\left(\frac{y}{\sqrt{\alpha_1\alpha_2\beta_{s1}\tilde{\beta}_{r1}}}\right), \tag{A.3}$$

where $K_1(\cdot)$ is the first order modified Bessel function of the second kind [43, eq. (8.432)]. With the obtained (A.3), $\mathcal{B}_1(\varepsilon_1)$ can be evaluated as

$$\mathcal{B}_1(\varepsilon_1) = 1 - \frac{2\gamma_{\text{th},1}}{\rho}\sqrt{\frac{\alpha_1\alpha_2}{\beta_{s1}\tilde{\beta}_{r1}}} e^{-\left(\frac{\alpha_2}{\tilde{\beta}_{r1}}+\frac{\alpha_1}{\beta_{s1}}\right)\frac{\gamma_{\text{th},1}}{\rho}} \times K_1\left(\frac{2\gamma_{\text{th},1}}{\rho}\sqrt{\frac{\alpha_1\alpha_2}{\beta_{s1}\tilde{\beta}_{r1}}}\right). \tag{A.4}$$

Similarly, we can evaluate $\mathcal{B}_2(\varepsilon_1)$ as

$$\mathcal{B}_2(\varepsilon_1) = 1 - \frac{2\gamma_{\text{th},2}}{\rho}\sqrt{\frac{\alpha_1\alpha_2}{\beta_{s2}\tilde{\beta}_{r2}}} e^{-\left(\frac{\alpha_2}{\tilde{\beta}_{r2}}+\frac{\alpha_1}{\beta_{s2}}\right)\frac{\gamma_{\text{th},2}}{\rho}} \times K_1\left(\frac{2\gamma_{\text{th},2}}{\rho}\sqrt{\frac{\alpha_1\alpha_2}{\beta_{s2}\tilde{\beta}_{r2}}}\right). \tag{A.5}$$

For $\mathcal{B}_1(\varepsilon_2)$ and $\mathcal{B}_1(\varepsilon_3)$, it can be easily shown that $\mathcal{B}_1(\varepsilon_2) = \mathcal{B}_1(\varepsilon_3) = 1 - e^{-\frac{\xi_1}{\beta_{s1}}}$. For $\mathcal{B}_2(\varepsilon_2)$ and $\mathcal{B}_2(\varepsilon_3)$, we have $\mathcal{B}_2(\varepsilon_2) = \mathcal{B}_2(\varepsilon_3)$, which can be evaluated by

$$\begin{aligned}\mathcal{B}_2(\varepsilon_i) &= \Pr\{|h_{s2}|^2 < \xi_1\} + \Pr\{|h_{s2}|^2 \geq \xi_1, |h_{s2}|^2 < \xi_2\} \\ &= 1 - e^{-\frac{\xi_1}{\beta_{s2}}} + \left[e^{-\frac{\xi_1}{\beta_{s2}}} - e^{-\frac{\xi_2}{\beta_{s2}}}\right]^+. \end{aligned} \tag{A.6}$$

Appendix B
A proof of Theorem 3

The end-to-end received SNR events at U_1 and U_2 can be summarized in Table VII. Based on the results in Table VII, the undetermined SNR events at U_1 can be classified into two types, i.e., $\{(33), \hat{\varepsilon}_2\}$ and $\{(36), \hat{\varepsilon}_2\}$. Regarding $\{(33), \hat{\varepsilon}_2\}$ and $\{(36), \hat{\varepsilon}_2\}$, we define

$$\hat{\mathcal{P}}_1 \triangleq \Pr\left\{\frac{\rho(\alpha_1|h_{s1}|^2 + |\tilde{h}_{r1}|^2)}{\alpha_2\rho|h_{s1}|^2 + 1} < \gamma_{\text{th},1}, \hat{\varepsilon}_2\right\} \tag{B.1}$$

and

$$\hat{\mathcal{P}}_2 \triangleq \Pr\left\{\frac{\alpha_1\rho(|h_{s1}|^2 + |\tilde{h}_{r1}|^2)}{\alpha_2\rho(|h_{s1}|^2 + |\tilde{h}_{r1}|^2) + 1} < \gamma_{\text{th},1}, \hat{\varepsilon}_2\right\}, \tag{B.2}$$

respectively. Since that all the channel gains follow exponential distributions, $\hat{\mathcal{P}}_1$ and $\hat{\mathcal{P}}_2$ can be respectively evaluated as

$$\begin{aligned}\hat{\mathcal{P}}_1 &= \Pr\left\{|h_{s1}|^2 < \xi_1\left(1 - \frac{\rho|\tilde{h}_{r1}|^2}{\gamma_{\text{th},1}}\right), |h_{s1}|^2 < \xi_1\right\} \\ &= \begin{cases} \dfrac{\beta_{s1}\gamma_{\text{th},1}\left(1 - e^{-\frac{\xi_1}{\beta_{s1}}}\right) - \tilde{\beta}_{r1}\rho\xi_1\left(1 - e^{-\frac{\gamma_{\text{th},1}}{\tilde{\beta}_{r1}\rho}}\right)}{\beta_{s1}\gamma_{\text{th},1} - \tilde{\beta}_{r1}\rho\xi_1}, \\ \qquad \beta_{s1} \neq \dfrac{\rho\tilde{\beta}_{r1}\xi_1}{\gamma_{\text{th},1}} \\ \gamma\left(2, \dfrac{\xi_1}{\beta_{s1}}\right), \quad \beta_{s1} = \dfrac{\rho\tilde{\beta}_{r1}\xi_1}{\gamma_{\text{th},1}} \end{cases}, \end{aligned} \tag{B.3}$$

and

$$\hat{\mathcal{P}}_2 = \Pr\Big\{|h_{s1}|^2 + |\tilde{h}_{r1}|^2 < \xi_1, |h_{s1}|^2 < \xi_1\Big\} = \begin{cases} \dfrac{\tilde{\beta}_{r1}\big(1 - e^{-\frac{\xi_1}{\tilde{\beta}_{r1}}}\big) - \beta_{s1}\big(1 - e^{-\frac{\xi_1}{\beta_{s1}}}\big)}{\tilde{\beta}_{r1} - \beta_{s1}}, & \beta_{s1} \neq \tilde{\beta}_{r1} \\ \gamma\big(2, \dfrac{\xi_1}{\beta_{s1}}\big), & \beta_{s1} = \tilde{\beta}_{r1}. \end{cases} \tag{B.4}$$

Then, regarding Table VII, the outage probability in (58) can be expressed as

$$\begin{aligned} P_{\text{out},1}^{\text{isdf}} &= \hat{\mathcal{P}}_1\big(\Pr\{\varepsilon_1\}\Pr\{\tilde{\varepsilon}_1\} + \Pr\{\varepsilon_2\}\Pr\{\tilde{\varepsilon}_1\} \\ &\quad + \Pr\{\varepsilon_2\}\Pr\{\tilde{\varepsilon}_2\} + \Pr\{\varepsilon_2\}\Pr\{\tilde{\varepsilon}_3\}\big) \\ &\quad + \hat{\mathcal{P}}_2\big(\Pr\{\varepsilon_1\}\Pr\{\tilde{\varepsilon}_2\} + \Pr\{\varepsilon_1\}\Pr\{\tilde{\varepsilon}_3\}\}\big) \\ &\quad + \Pr\{\varepsilon_3\}\big(\Pr\{\hat{\varepsilon}_2\}\Pr\{\tilde{\varepsilon}_1\} + \Pr\{\hat{\varepsilon}_2\}\Pr\{\tilde{\varepsilon}_2\} \\ &\quad + \Pr\{\hat{\varepsilon}_2\}\Pr\{\tilde{\varepsilon}_3\}\big) \\ &= \hat{\mathcal{P}}_1\big(\Pr\{\varepsilon_1\}\Pr\{\tilde{\varepsilon}_1\} + \Pr\{\varepsilon_2\}\big) \\ &\quad + \hat{\mathcal{P}}_2\Pr\{\varepsilon_1\}\big(1 - \Pr\{\tilde{\varepsilon}_1\}\big) + \Pr\{\varepsilon_3\}\Pr\{\hat{\varepsilon}_2\}, \end{aligned} \tag{B.5}$$

which proves the case for U_1.

According to Table VII, the undetermined SNR events at U_2 can be classified into four types, i.e., $\{(29), \tilde{\varepsilon}_2\}$, $\{(31), (32), \tilde{\varepsilon}_3\}$, $\{(32), \tilde{\varepsilon}_2\}$, and $\{(38), (39), \tilde{\varepsilon}_3\}$. With respect to these four types of the undetermined SNR events, we define

$$\widetilde{\mathcal{P}}_1 \triangleq \Pr\{\rho(\alpha_2|h_{s2}|^2 + |\tilde{h}_{r2}|^2) < \gamma_{\text{th},2}, \tilde{\varepsilon}_2\}, \tag{B.6}$$

$$\begin{aligned} \widetilde{\mathcal{P}}_2 \triangleq \Pr\Big\{\frac{\alpha_1\rho(|h_{s2}|^2 + |\tilde{h}_{r2}|^2)}{\alpha_2\rho(|h_{s2}|^2 + |\tilde{h}_{r2}|^2) + 1} < \gamma_{\text{th},1}, \tilde{\varepsilon}_3\Big\} \\ + \Pr\Big\{\frac{\alpha_1\rho(|h_{s2}|^2 + |\tilde{h}_{r2}|^2)}{\alpha_2\rho(|h_{s2}|^2 + |\tilde{h}_{r2}|^2) + 1} \geq \gamma_{\text{th},1}, \\ \alpha_2\rho(|h_{s2}|^2 + |\tilde{h}_{r2}|^2) < \gamma_{\text{th},2}, \tilde{\varepsilon}_3\Big\}, \end{aligned} \tag{B.7}$$

$$\widetilde{\mathcal{P}}_3 \triangleq \Pr\{\alpha_2\rho(|h_{s2}|^2 + |\tilde{h}_{r2}|^2) < \gamma_{\text{th},2}, \tilde{\varepsilon}_2\}, \tag{B.8}$$

and

$$\begin{aligned} \widetilde{\mathcal{P}}_4 \triangleq \Pr\Big\{\frac{\rho(\alpha_1|h_{s2}|^2 + |\tilde{h}_{r2}|^2)}{\alpha_2\rho|h_{s2}|^2 + 1} < \gamma_{\text{th},1}, \tilde{\varepsilon}_3\Big\} \\ + \Pr\Big\{\frac{\rho(\alpha_1|h_{s2}|^2 + |\tilde{h}_{r2}|^2)}{\alpha_2\rho|h_{s2}|^2 + 1} \geq \gamma_{\text{th},1}, \\ \alpha_2\rho|h_{s2}|^2 < \gamma_{\text{th},2}, \tilde{\varepsilon}_3\Big\}, \end{aligned} \tag{B.9}$$

respectively. Taking into account that all the channel gains follow exponential distributions, $\widetilde{\mathcal{P}}_1$, $\widetilde{\mathcal{P}}_2$, $\widetilde{\mathcal{P}}_3$, and $\widetilde{\mathcal{P}}_4$ can be respectively evaluated as those in Table VI. As such, the outage probability at U_2 can be expressed as (66).

REFERENCES

[1] Y. Saito, A. Benjebbour, Y. Kishiyama, and T. Nakamura, "System-level performance evaluation of downlink non-orthogonal multiple access (NOMA)," in *Proc. IEEE 24th PIMRC*, London, U.K., Sep. 2013, pp. 611–615.

[2] Z. Ding, M. Peng, and H. V. Poor, "Cooperative non-orthogonal multiple access in 5G systems," *IEEE Commun. Lett.*, vol. 19, no. 8, pp. 1462–1465, Aug. 2015.

[3] S. M. R. Islam, N. Avazov, O. A. Dobre, and K.-S. Kwak, "Power-domain non-orthogonal multiple access (NOMA) in 5G systems: Potentials and challenges," *IEEE Commun. Surveys Tuts.*, vol. 19, no. 2, pp. 721–742, 2nd Quart., 2017.

[4] A. E. Mostafa, Y. Zhou, and V. W. S. Wong, "Connectivity maximization for narrowband IoT systems with NOMA," in *Proc. IEEE ICC*, Paris, France, May 2017, pp. 1–6.

[5] *Study on Downlink Multiuser Superposition Transmission for LTE*, document RP-150496, TSG RAN Meeting 67, 3rd Geneartion Partnership Project, Mar. 2015.

[6] Y. Yuan *et al.*, "Non-orthogonal transmission technology in LTE evolution," *IEEE Commun. Mag.*, vol. 54, no. 7, pp. 68–74, Jul. 2016.

[7] Z. Ding, Z. Yang, P. Fan, and H. V. Poor, "On the performance of non-orthogonal multiple access in 5G systems with randomly deployed users," *IEEE Signal Process. Lett.*, vol. 21, no. 12, pp. 1501–1505, Dec. 2014.

[8] S. Timotheou and I. Krikidis, "Fairness for non-orthogonal multiple access in 5G systems," *IEEE Signal Process. Lett.*, vol. 22, no. 10, pp. 1647–1651, Oct. 2015.

[9] Z. Yang, Z. Ding, P. Fan, and G. K. Karagiannidis, "On the performance of non-orthogonal multiple access systems with partial channel information," *IEEE Trans. Commun.*, vol. 64, no. 2, pp. 654–667, Feb. 2016.

[10] Z. Ding *et al.*, "Impact of user pairing on 5G nonorthogonal multiple-access downlink transmissions," *IEEE Trans. Veh. Technol.*, vol. 65, no. 8, pp. 6010–6023, Aug. 2016.

[11] J. Men and J. Ge, "Non-orthogonal multiple access for multiple-antenna relaying networks," *IEEE Commun. Lett.*, vol. 19, no. 10, pp. 1686–1689, Oct. 2015.

[12] J. Men, J. Ge, and C. Zhang, "Performance analysis of non-orthogonal multiple access for relaying networks over Nakagami-m fading channels," *IEEE Trans. Veh. Technol.*, vol. 66, no. 2, pp. 1200–1208, Feb. 2017.

[13] J. Men, J. Ge, and C. Zhang, "Performance analysis for downlink relaying aided non-orthogonal multiple access networks with imperfect CSI over Nakagami-m fading," *IEEE Access*, vol. 5, pp. 998–1004, Nov. 2016.

[14] S. Lee, D. B. da Costa, and T. Q. Duong, "Outage probability of non-orthogonal multiple access schemes with partial relay selection," in *Proc. IEEE 26th PIMRC*, Valencia, Spain, Sep. 2016, pp. 1–6.

[15] Z. Yang, Z. Ding, Y. Wu, and P. Fan, "Novel relay selection strategies for cooperative NOMA," *IEEE Trans. Veh. Technol.*, vol. 66, no. 11, pp. 10114–10123, Nov. 2017.

[16] Z. Ding, H. Dai, and H. V. Poor, "Relay selection for cooperative NOMA," *IEEE Wireless Commun. Lett.*, vol. 5, no. 4, pp. 416–419, Aug. 2016.

[17] X. Liu and X. Wang, "Outage probability and capacity analysis of the collaborative NOMA assisted relaying system in 5G," in *Proc. IEEE/CIC Int. Conf. Commun. China (ICCC)*, Chengdu, China, Jul. 2016, pp. 1–5.

[18] C. Zhong and Z. Zhang, "Non-orthogonal multiple access with cooperative full-duplex relaying," *IEEE Commun. Lett.*, vol. 20, no. 12, pp. 2478–2481, Dec. 2016.

[19] Z. Zhang, Z. Ma, M. Xiao, Z. Ding, and P. Fan, "Full-duplex device-to-device aided cooperative non-orthogonal multiple access," *IEEE Trans. Veh. Technol.*, vol. 66, no. 5, pp. 4467–4471, May 2017.

[20] X. Yue, Y. Liu, S. Kang, A. Nallanathan, and Z. Ding, "Outage performance of full/half-duplex user relaying in NOMA systems," in *Proc. IEEE ICC*, Paris, France, May 2017, pp. 1–6.

[21] L. Zhang, J. Liu, M. Xiao, G. Wu, Y.-C. Liang, and S. Li, "Performance analysis and optimization in downlink NOMA systems with cooperative full-duplex relaying," *IEEE J. Sel. Areas Commun.*, vol. 35, no. 10, pp. 2398–2412, Oct. 2017.

[22] Y. Liu, Z. Ding, M. Elkashlan, and H. V. Poor, "Cooperative non-orthogonal multiple access with simultaneous wireless information and power transfer," *IEEE J. Sel. Areas Commun.*, vol. 34, no. 4, pp. 938–953, Apr. 2016.

[23] N. T. Do, D. B. da Costa, T. Q. Duong, and B. An, "A BNBF user selection scheme for NOMA-based cooperative relaying systems with SWIPT," *IEEE Commun. Lett.*, vol. 21, no. 3, pp. 664–667, Mar. 2017.

[24] J.-B. Kim and I.-H. Lee, "Non-orthogonal multiple access in coordinated direct and relay transmission," *IEEE Commun. Lett.*, vol. 19, no. 11, pp. 2037–2040, Nov. 2015.

[25] J.-B. Kim, I.-H. Lee, and J. Lee, "Capacity scaling for D2D aided cooperative relaying systems using NOMA," *IEEE Commun. Lett.*, vol. 7, no. 1, pp. 42–45, Feb. 2018.

[26] S.-N. Hong and G. Caire, "Reverse compute and forward: A low-complexity architecture for downlink distributed antenna systems," in *Proc. IEEE ISIT*, Cambridge, MA, USA, Jul. 2012, pp. 1147–1151.

[27] M. El Soussi, A. Zaidi, and L. Vandendorpe, "Compute-and-forward on a multiaccess relay channel: Coding and symmetric-rate optimization," *IEEE Trans. Wireless Commun.*, vol. 13, no. 4, pp. 1932–1947, Apr. 2014.

[28] M. E. Soussi, A. Zaidi, and L. Vandendorpe, "Compute-and-forward on a multi-user multi-relay channel," *IEEE Wireless Commun. Lett.*, vol. 3, no. 6, pp. 589–592, Dec. 2014.

[29] T.-Y. Tseng, C.-P. Lee, S.-C. Lin, and H.-J. Su, "Non-orthogonal compute-and-forward with joint lattice decoding for the multiple-access relay channel," in *Proc. IEEE Globecom Workshops (GC Wkshps)*, Austin, TX, USA, Dec. 2014, pp. 924–929.

[30] I. Estella-Aguerri and A. Zaidi, "Lossy compression for compute-and-forward in limited backhaul uplink multicell processing," *IEEE Trans. Commun.*, vol. 64, no. 12, pp. 5227–5238, Dec. 2016.

[31] M. N. Hasan and B. M. Kurkoski, "Practical compute-and-forward approaches for the multiple access relay channel," in *Proc. IEEE Int. Conf. Commun. (ICC)*, Paris, France, May 2017, pp. 1–6.

[32] F. A. Onat, A. Adinoyi, Y. Fan, H. Yanikomeroglu, and J. Thompson, "Optimum threshold for SNR-based selective digital relaying schemes in cooperative wireless networks," in *Proc. IEEE WCNC*, Hong Kong, Mar. 2007, pp. 969–974.

[33] F. A. Onat, A. Adinoyi, Y. Fan, H. Yanikomeroglu, J. S. Thompson, and I. D. Marsland, "Threshold selection for SNR-based selective digital relaying in cooperative wireless networks," *IEEE Trans. Wireless Commun.*, vol. 7, no. 11, pp. 4226–4237, Nov. 2008.

[34] J. N. Laneman, D. N. C. Tse, and G. W. Wornell, "Cooperative diversity in wireless networks: Efficient protocols and outage behavior," *IEEE Trans. Inf. Theory*, vol. 50, no. 12, pp. 3062–3080, Dec. 2004.

[35] B. Zhao and M. C. Valenti, "Practical relay networks: A generalization of hybrid-ARQ," *IEEE J. Sel. Areas Commun.*, vol. 23, no. 1, pp. 7–18, Jan. 2005.

[36] S. Ikki and M. H. Ahmed, "Performance analysis of incremental relaying cooperative diversity networks over Rayleigh fading channels," *IET Commun.*, vol. 5, no. 3, pp. 337–349, Feb. 2011.

[37] H. Chen, J. Liu, C. Zhai, and Y. Liu, "Performance of incremental-selective decode-and-forward relaying cooperative communications over Rayleigh fading channels," in *Proc. IEEE WCSP*, Nanjing, China, Nov. 2009, pp. 1–6.

[38] T. T. Duy and H.-Y. Kong, "Performance analysis of hybrid decode-amplify-forward incremental relaying cooperative diversity protocol using SNR-based relay selection," *J. Commun. Netw.*, vol. 14, no. 6, pp. 703–709, Dec. 2012.

[39] Z. Bai, J. Jia, C.-X. Wang, and D. Yuan, "Performance analysis of SNR-based incremental hybrid decode-amplify-forward cooperative relaying protocol," *IEEE Trans. Commun.*, vol. 63, no. 6, pp. 2094–2106, Jun. 2015.

[40] Y. Feng, S. Yan, Z. Yang, N. Yang, and W.-P. Zhu, "TAS-based incremental hybrid decode–amplify–forward relaying for physical layer security enhancement," *IEEE Trans. Commun.*, vol. 63, no. 9, pp. 3876–3891, Sep. 2017.

[41] V. Tarokh, H. Jafarkhani, and A. R. Calderbank, "Space-time block codes from orthogonal designs," *IEEE Trans. Inf. Theory*, vol. 45, no. 5, pp. 1456–1467, Jul. 1999.

[42] M. O. Hasna and M.-S. Alouini, "Performance analysis of two-hop relayed transmissions over Rayleigh fading channels," in *Proc. IEEE 56th VTC*, Vancouver, BC, Canada, Sep. 2002, pp. 1992–1996.

[43] I. S. Gradshteyn and I. M. Ryzhik, *Table of Integrals, Series, and Products*. New York, NY, USA: Academic, 2007.

Hongwu Liu received the Ph.D. degree from Southwest Jiaotong University in 2008. From 2008 to 2010, he was with Nanchang Hangkong University. From 2010 to 2011, he was a Post-Doctoral Fellow with the Shanghai Institute of Microsystem and Information Technology, Chinese Academy of Science. From 2011 to 2013, he was a Research Fellow with the UWB Wireless Communications Research Center, Inha University, South Korea. From 2017 to 2018, he was a Research Professor with the Department of Information and Communication Engineering, Inha University. Since 2014, he has been an Associate Professor with Shandong Jiaotong University. His research interests include MIMO signal processing, cognitive radios, cooperative communications, wireless secrecy communications, and 5G networks.

Zhiguo Ding (SM'15) received the B.Eng. degree in electrical engineering from the Beijing University of Posts and Telecommunications in 2000 and the Ph.D. degree in electrical engineering from Imperial College London in 2005. From 2005 to 2018, he was with Queen's University Belfast, Imperial College London, Newcastle University, and Lancaster University. Since 2018, he has been a Professor in communications with The University of Manchester. From 2012 to 2018, he was an Academic Visitor with Princeton University.

His research interests are 5G networks, game theory, cooperative and energy harvesting networks, and statistical signal processing. He received the Best Paper Award from IET ICWMC 2009 and the IEEE WCSP 2014, the EU Marie Curie Fellowship from 2012 to 2014, the Top IEEE TVT Editor 2017, the IEEE Heinrich Hertz Award 2018, and the IEEE Jack Neubauer Memorial Award 2018. He was an Editor for the *IEEE Wireless Communication Letters*, the IEEE COMMUNICATIONS LETTERS from 2013 to 2016. He is serving as an Editor for the IEEE TRANSACTIONS ON COMMUNICATIONS, the IEEE TRANSACTIONS ON VEHICULAR TECHNOLOGY, and the *Journal of Wireless Communications and Mobile Computing*.

Kyeong Jin Kim (SM'11) received the M.S. degree from the Korea Advanced Institute of Science and Technology in 1991 and the M.S. and Ph.D. degrees in electrical and computer engineering from the University of California at Santa Barbara, Santa Barbara, CA, USA, in 2000. From 1991 to 1995, he was a Research Engineer with the Video Research Center, Daewoo Electronics Ltd., South Korea. In 1997, he joined the Data Transmission and Networking Laboratory, University of California at Santa Barbara. After receiving his degrees, he joined the Nokia Research Center and Nokia Inc., Dallas, TX, USA, as a Senior Research Engineer, where he was an L1 Specialist, from 2005 to 2009. From 2010 to 2011, he was an Invited Professor with Inha University, South Korea. Since 2012, he has been a Senior Principal Research Staff with Mitsubishi Electric Research Laboratories, Cambridge, MA, USA. His research interests include transceiver design, resource management, scheduling in cooperative wireless communications systems, cooperative spectrum sharing systems, physical layer secrecy systems, and device-to-device communications.

Dr. Kim served as an Editor for the IEEE COMMUNICATIONS LETTERS and the *International Journal of Antennas and Propagation*. He also served as a Guest Editor for the *EURASIP Journal on Wireless Communications and Networking* Special Issue on Cooperative Cognitive Networks and *IET Communications* Special Issue on Secure Physical Layer Communications. He currently serves as an Editor for the IEEE TRANSACTIONS ON COMMUNICATIONS and as a leading Guest Editor for the IEEE JOURNAL ON SELECTED AREAS IN COMMUNICATIONS SPECIAL ISSUE ON HARDWARE FRIENDLY SPATIAL MODULATION IN EMERGING WIRELESS SYSTEMS.

Kyung Sup Kwak received the Ph.D. degree from the University of California at San Diego, and worked for Hughes Network Systems and the IBM Network Analysis Center, USA. He was with the School of Information and Communication Engineering, Inha University, South Korea, as a Professor, and has been the Dean of the Graduate School of Information Technology and Telecommunications and the Director of the UWB Wireless Communications Research Center, an IT research center, South Korea, since 2003. In 2006, he served as the President of the Korean Institute of Communication Sciences (KICS) and as the President of the Korea Institute of Intelligent Transport Systems (KITS) in 2009. In 2008, he was elected as an Inha Fellow Professor and currently as an Inha Hanlim Fellow Professor. He has published over 200 peer-reviewed journal papers. His research interests include multiple access communication systems, mobile and UWB radio systems, future IoT, and wireless body area networks: nano networks and molecular communications. In 1993, he received the Engineering College Achievement Award from Inha University and the Service Award from the Institute of Electronics Engineers of Korea. In 1996 and 1999, he received the Distinguished Service Awards from the KICS. He received the LG Paper Award in 1998 and the Motorola Paper Award in 2000. He received official commendations for UWB radio technology research and development from the Minister of Information and Communication, the Prime Minister, and the President of South Korea in 2005, 2006, and 2009, respectively. In 2007, he received the Haedong Paper Award and the Haedong Scientific Award of research achievement in 2009. He served as the TPC chair and the track chair/organizing chair for several IEEE-related conferences.

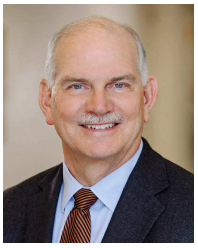

H. Vincent Poor (S'72–M'77–SM'82–F'87) received the Ph.D. degree in EECS from Princeton University in 1977. From 1977 until 1990, he was on the faculty of the University of Illinois at Urbana-Champaign. Since 1990 he has been on the faculty at Princeton, where he is currently the Michael Henry Strater University Professor of Electrical Engineering. During 2006 to 2016, he served as Dean of Princeton's School of Engineering and Applied Science. He has also held visiting appointments at several other universities, including most recently at Berkeley and Cambridge. His research interests are in the areas of information theory and signal processing, and their applications in wireless networks, energy systems and related fields. Among his publications in these areas is the recent book *Information Theoretic Security and Privacy of Information Systems* (Cambridge University Press, 2017).

Dr. Poor is a member of the National Academy of Engineering and the National Academy of Sciences, and is a foreign member of the Chinese Academy of Sciences, the Royal Society, and other national and international academies. He received the Marconi and Armstrong Awards of the IEEE Communications Society in 2007 and 2009, respectively. Recent recognition of his work includes the 2017 IEEE Alexander Graham Bell Medal, Honorary Professorships at Peking University and Tsinghua University, both conferred in 2017, and a D.Sc. *(honoris causa)* from Syracuse University also awarded in 2017.